Akademia Górniczo-Hutnicza

University of Science and Technology

Final project

FATIGUE AND FRACTURE BEHAVIOR OF COMPOSITES WITH METAL MATRIX

Author: Verónica Torrijos Berlanas

Project tutor: Ryszard Pecherski

Acknowledgements

First I want to thank my parents, Antonio and Gloria, and brothers, Sergio and Natalia, for helping me in everything that they could.

Also I would like to thank the support received from my friends, for they have beared my nerves with the exams, especially Isabel and Patricia, without you the university would not have been the same.

In closing I want to thank for the assistance given to Carlos Santiuste, and to Ryszard Pecherski the opportunity that he has given me for do my final project.

Thanks everybody.

TABLE OF CONTENT

1. Resumen

Los materiales compuestos son un sistema formado por una mezcla o composición de dos o más micro - macro constituyentes que difieren en forma y composición química y son insolubles entre sí.

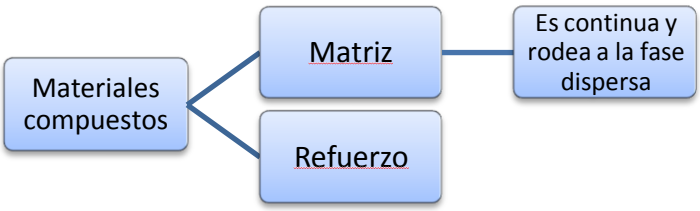

Las funciones de la matriz en un material compuesto son:

- Mantener la armadura en la posición de trabajo y distribuir la carga entre ellos.
- Proteger el refuerzo del deterioro mecánico y químico.
- Evitar la propagación de grietas.

Los tipos de matriz son:

Metálica:

- Los materiales compuestos tienen una alta resistencia y bajo peso.
- Se mejora el comportamiento a la fluencia de la aleación base, se pueden obtener propiedades de direccionalidad: este aumento de la resistencia está asociada con una disminución en la tenacidad de la aleación.

Cerámica:

- Estos compuestos tienen mejores propiedades mecánicas como la dureza y resistencia de los materiales cerámicos tradicionales, especialmente en la gama de baja temperatura.

Polimérica:

- Buenas propiedades mecánicas, resistencia a la corrosión y agentes químicos.

Refuerzos.

Los materiales compuestos también se pueden clasificar de acuerdo con el tipo de refuerzo. Las propiedades del material compuesto se basan en las propiedades de las fases constituyentes, sus proporciones relativas y la geometría de la armadura, la forma, tamaño, distribución y orientación.

Hay dos tipos de refuerzos:

1. Refuerzos continuos.

- Fibras de vidrio: Buena resistencia mecánica y buena resistencia al peso.
- Fibras de carbono: Muy ligeras y con baja densidad.
- Fibras orgánicas: Alta resistencia y alto modulo de elasticidad.
- Fibras cerámicas: Alta resistencia y una buena relación del módulo elástico a alta temperatura.
- Fibras de boro: El boro es un material frágil.

2. Refuerzos discontinuos.

- Whiskers: Se proporciona oportunidades para reducir los costes de operación en el ciclo de vida de muchas aplicaciones de peso crítico. Tienen la desventaja de no tener un tamaño uniforme.
- Partículas: El refuerzo es mucho más eficaz, cuando las partículas son pequeñas y se distribuyen homogéneamente en la matriz. Las propiedades mecánicas mejoran con el aumento del contenido de partículas, son relativamente baratos.
- Fibras cortas: Buen nivel de rendimiento mecánico con un coste relativamente bajo.

Efectos del refuerzo.

En los materiales compuestos, las propiedades mecánicas dependen del número, tamaño, forma y distribución de la fase dispersa, además de las propiedades mecánicas de la matriz y la naturaleza de la interfaz.

Ventajas:

- Alta resistencia y rigidez.
- Mejor comportamiento a alta temperatura, que muestran una mayor resistencia y una mejor resistencia a la fluencia.
- Bajo coeficiente de expansión térmica, en general, en función del refuerzo.
- Resistencia a la fatiga a través del uso de ciertas fibras.

Materiales compuestos con matriz metálica.

Los compuestos de matriz metálica contienen refuerzos cerámicos en una matriz de aleación metálica. La matriz puede ser una aleación de Al o Ti, mientras que los refuerzos pueden ser Al_2O_3 o SiC.

Los compuestos de matriz metálica reforzados con partículas son los más económicos y los más populares. Estos compuestos ofrecen una mayor rigidez, resistencia a temperatura elevada y resistencia al desgaste

Comportamiento a fractura.

Análisis elástico.

Depende de las expresiones para la división de la tensión y la deformación en las dos fases.

La tensión o la deformación pueden ser asumidas para ser igual en las dos fases:

- Durante la deformación axial de los materiales compuestos reforzados continuamente (límite superior) la igualdad de tensión (el modelo de Voigt) aparece.

- La igualdad de la tensión de fase (el modelo Reuss) se desarrolla durante la deformación transversal de laminados compuestos (límite inferior).

Para la cota superior:

La tensión del material compuesto (σ_a^c) y la deformación (ε_a^c) en la dirección axial se pueden escribir en términos de la deformación y la tensión en la matriz (σ_a^m, ε_a^m) y refuerzo (σ_a^r, ε_a^r) y la fracción de volumen de la fase de refuerzo (f).

$$\sigma_a^c = (1-f)\sigma_a^m + f\sigma_a^r$$

$$\varepsilon_a^c = \varepsilon_a^m = \varepsilon_a^r$$

Para el borde inferior:

$$\varepsilon_t^c = (1-f)\varepsilon_t^m + f\varepsilon_t^r$$

$$\sigma_t^c = \sigma_t^m = \sigma_t^r$$

Para MMCs reforzados de forma discontinua, las tensiones y las deformaciones en las dos fases pueden ser diferentes.

Análisis elastoplástico.

Para las bajas fracciones en volumen de inclusiones rígidas en una matriz de plástico el efecto global de las inclusiones en la deformación del material compuesto sería pequeña.

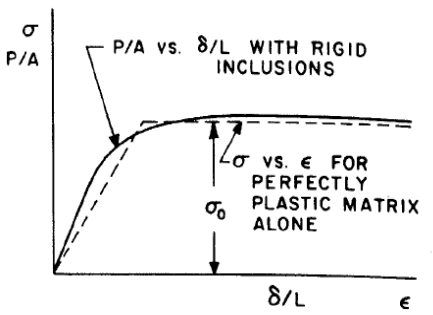

Sin embargo, para el endurecimiento por deformación de la matriz, la presencia de las inclusiones bloquearía el deslizamiento de los planos.

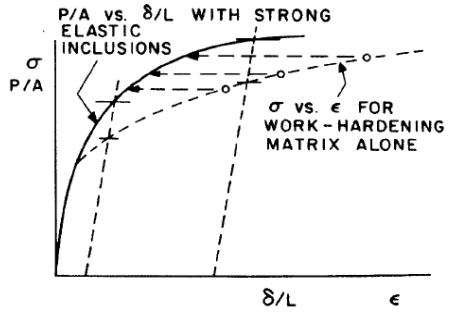

Dependiendo de la escala de longitud del modelo, estos estudios se dividen principalmente en dos categorías:

- Los modelos autoconsistentes.
- Los modelos micromecánicos (elementos finitos).

Modelos de auto-consistentes (campo medio).

Los modelos de auto-consistentes calculan el promedio (o media) de las tensiones en la fase entre el refuerzo y la matriz. Tratan estas fases como si se insertan en un medio infinito (compuesto eficaz), y determinan sus características de deformación por el método Eshelby.

La tensión en los refuerzos (σ^p) y la matriz (σ^m) están dados por:

$$\sigma^p = C_p\left(SC_p + (1-S)C_c\right)^{-1}\sigma^A$$

$$\sigma^m = C_m(SC_m + (1-S)C_c)^{-1}\sigma^A$$

Donde C_p, C_m y C_c son la rigidez de la armadura, y la matriz de material compuesto, respectivamente, S es el tensor de Eshelby y σ^A es la tensión aplicada.

El análisis anterior supone una distribución uniforme de los refuerzos.

Micromecánica (modelos de elementos finitos).

Los modelos de elementos finitos son muy adecuados para el modelado de la tensión local / campos de deformación de los procesos de deformación de material compuesto.

- El método consiste en discretizar el continuo en un número finito de elementos, cuya deformación se puede caracterizar en términos de un número finito de parámetros.
- Cada elemento se le asigna propiedades características de los materiales de las propiedades de cualquiera de las fases de la matriz o del refuerzo, dependiendo de la fase del elemento que representa. La solución de elementos finitos implica la búsqueda de un campo de desplazamiento de la fuerza lo que minimiza la energía total del dominio.

Formación de microdaños causados por la deformación.

La rotura de la MMC se produce por un proceso de nucleación, crecimiento y coalescencia de huecos.

La nucleación de cavidades en el material se puede producir:

- Por rotura dúctil de la matriz.
- Descohesión de la interfaz de la matriz-refuerzo.
- Rotura refuerzo cerámico frágil.

Formación de huecos en la matriz.

La fractura dúctil de la matriz es el mecanismo de fallo observado en aleaciones basadas en MMC donde aparecen intermetálicos con un tamaño del orden de varias micras.

Estas fases son normalmente debido a la presencia de impurezas tales como hierro en la composición de la matriz y son sitios preferenciales para la nucleación de cavidades.

En el caso del mecanismo de tensión controlada, la velocidad de crecimiento disminuye después de la nucleación porque la tensión hidrostática puede ser aliviada por una gran cantidad de vacío de nucleación.

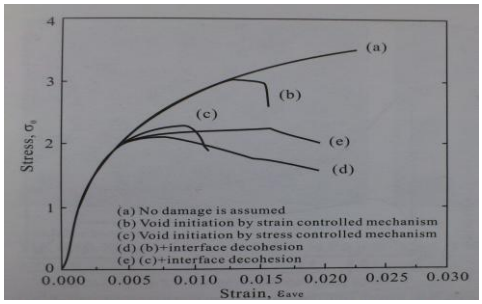

Fractura de refuerzo.

El mecanismo de fallo observado en los materiales de refuerzo cerámico normalmente es la fractura frágil.

Las tensiones que actúan sobre el material de refuerzo durante la deformación pueden exceder de la resistencia mecánica de las partículas cerámicas, lo que resulta en rotura frágil de refuerzo antes de aparecer cavidades en la interfaz de la matriz-refuerzo.

Desunión de la interfaz.

Es el mecanismo de ruptura por lo general se observa en MMC reforzado con whiskers.

- Los extremos de los whiskers actúan como concentradores de tensiones.
- La descohesión de refuerzo también se ve influida por los procesos de precipitación en el material.
- La aparición de fases estables en la interfase matriz-refuerzo promueve la nucleación de huecos en los extremos de la armadura.
- La interfaz de desunión se produce cuando la tensión de cizallamiento local de τ interfaz o el esfuerzo vertical excede la resistencia de la zona de interfase.

Proceso de fractura

Proceso de fractura (evolución del daño y la coalescencia).

Si el vacío de nucleación está suficientemente lejos, el proceso de evolución del daño por cada vacío será bastante independiente de los otros y puede ser diferenciado en dos distintos.

(a) un crecimiento nulo

(b) sin efecto de coalescencia

Si el vacío nucleación no es lo suficientemente largo:

La nucleación de un vacío garantiza una reorientación de los campos de esfuerzo / deformaciones locales de todo el daño: la partícula dañada ya no puede soportar la carga previa y la carga adicional tienen que ser redistribuidos entre las partículas vecinas intactas y la matriz.

Dos reglas aproximadas se han definido para el trabajo en este campo:

- El mecanismo mundial de la carga compartida (GLS): (El fallo de una sola fibra no causa las concentraciones de esfuerzos importantes en las fibras vecinas, el fracaso de cada fibra es independiente de la del otro).
- El mecanismo de intercambio de carga local (LLS): (Se caracteriza por la alta concentración de esfuerzos debido a una fibra rota que conduce a fallo prematuro de las fibras vecinas).

Modo de crecimiento de grieta bajo carga monolítica.

La presencia del refuerzo cerámico en la MMC modifica su comportamiento mecánico, el aumento de la resistencia y la reducción de la ductilidad.

Los efectos de los factores físicos de cada tipo de grieta son:

Grieta de resistencia a la iniciación:

- Deformación cerca de la punta de la grieta (embotamiento, apertura).
- Ángulo de desviación antes de la extensión de la fisura.

El estrés de refuerzo

- Cambio de la singularidad de la tensión con extensión de la fisura.
- Cambio de la singularidad de la tensión de la grieta principal que cruza otra interfaz.
- Efecto de la zona plástica secundaria en la periferia del refuerzo.

La figura muestra un resumen esquemático de un modelo de crecimiento de la grieta general de aleación de aluminio de la matriz DRM. A: la deformación en la zona plástica, B: cambio de la singularidad de la tensión con extensión de la fisura, C: rotura de refuerzo, D: concentración de tensión en el extremo de refuerzo, E: descohesión y la formación de microgrietas, F: desviación de la grieta principales a lo largo de la ruta de acceso de microfisuras.

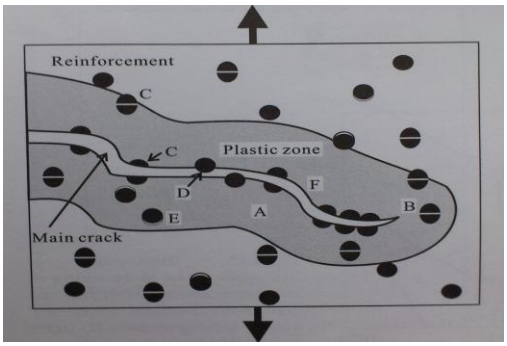

Deformación elástica.

Los factores que controlan el aumento de módulo de Young son la fracción de volumen de refuerzo y la forma de las partículas de cerámica.

Cuanto mayor sea el contenido de refuerzo mayor será la carga sobre las partículas de cerámica y por lo tanto más altos los módulos de Young.

La transferencia de la carga de la matriz de refuerzo es más eficaz cuanto más alargada son las partículas cerámicas.

Como resultado, el aumento del módulo elástico es mayor para refuerzos alargados, tales como whiskers, que para las partículas con un factor de forma próximo a la unidad.

Deformación plástica.

La deformación plástica de la tarjeta MMC está fuertemente influenciada por las propiedades de la matriz.

Los diferentes elementos de aleación en la matriz, así como los tratamientos térmicos son determinantes en el factor de resistencia, el rendimiento y la resistencia a la tracción de los compuestos.

La resistencia mecánica de los MMC, aumenta en relación a medir aleaciones no reforzadas, aunque el aumento en el límite elástico se reduce por el aumento de la resistencia de la matriz

Microestructura.

Factor microestructural de refuerzo.

Los parámetros que caracterizan las microestructuras de la armadura desde el punto de vista de su comportamiento mecánico son:

- Las características de la población de partículas (fracción de volumen, forma, tamaño, esbeltez, y la orientación de las partículas de refuerzo).
- La distribución espacial de la armadura (uniformidad o la presencia de agrupaciones o racimos de partículas).
- La distribución espacial de las partículas de refuerzo en la matriz, pueden afectar en algunas de las propiedades mecánicas del compuesto (límite de elasticidad, ductilidad ...) como en el proceso de localización de la deformación y el daño durante la deformación mecánica.
- Pueden esperarse propiedades mecánicas mejoradas mediante la eliminación de las partículas gruesas del refuerzo.

Factor microestructural sobre las interfaces.

- Cuando el módulo elástico de refuerzo es menor que el de la matriz, el refuerzo tiende a fallar como resultado de la creciente presión interna. Por lo tanto, se concluyó que un módulo elástico medio es deseable.

Factor microestructural sobre la matriz.

- En general, la tensión residual causada por la diferencia en el coeficiente de expansión térmica entre el refuerzo y la matriz influye fuertemente en la fuerza o resistencia de MMC.
- Se sabe que el mecanismo de daño y tenacidad a la fractura pueden ser en gran medida influenciados por la edad de endurecimiento para MMC.

- Por otro lado, una notable disminución de la resistencia es inducida porque la nucleación de vacío y el crecimiento son promovidos por la existencia de la matriz alterada.

Tensión residual

La magnitud de las tensiones residuales depende:

- La fracción de volumen de refuerzo.
- El tamaño y la geometría.
- Las temperaturas inicial y final del proceso.
- La velocidad de enfriamiento.

Las tensiones residuales influyen en el comportamiento mecánico de MMC, pueden alterar los valores de:

- La resistencia a la fluencia.
- Tenacidad.
- Resistencia a la fatiga.

Comportamiento a fatiga.

Mecanismo de deformación.

Cuando un material se prueba en función del ciclo, la tensión requerida para alcanzar la deformación impuesta varía a lo largo del proceso de deformación en función del ciclo.

El comportamiento bajo carga cíclica es muy sensible a los factores de microestructura.

Las aleaciones endurecidas por precipitados, se endurecen rápidamente durante la deformación cíclica.

En los materiales comprendidos a temperatura ambiente se puede ver un importante endurecimiento por deformación cíclica, mientras que los materiales comprendidos a alta temperatura tienen un comportamiento estable o incluso se pueden ver ablandamiento por deformación cíclica.

Estas deformaciones plásticas se concentran inicialmente en la interfaz de la matriz-refuerzo, que se extiende progresivamente a la matriz.

Mecanismo de fallo

Cuando un material es sometido a la acción de la carga cíclica la rotura se produce para valores de la tensión más baja que los que causan la ruptura del material cuando se producen con la carga monótona.

Cuando MMC, están sujetas a ciclos de amplitud de alta tensión la ruptura se produce bruscamente por mecanismos similares a los descritos mediante el análisis de la fisuración bajo tensión de carga monótona: fractura dúctil de la matriz, descohesión de la interfaz de la matriz-refuerzo o fractura frágil de la armadura de cerámica.

Microestructura

Hay dos tipos de fractura:

- Fractura corta
- Fractura larga

Grieta corta por fatiga:

Se llama una grieta corta microestructural cuando el tamaño de la grieta está en el mismo orden de la microestructura debido a la deformación de deslizamiento en una punta de la grieta está fuertemente influenciada por la microestructura.

La propagación de grietas con frecuencia disminuye o detenciones a causa de la interacción entre la microestructura y la grieta principal.

Grieta larga por fatiga

Las partículas de gran diámetro causan atrapamiento de fisura efectiva y aumentan el grado de desviación grieta al mismo tiempo aumentar el nivel de cierre de grieta.

Es necesario elegir el tamaño refuerzo cuidadosamente debido a que la directriz será muy diferente según el lugar donde se hará hincapié entre las propiedades del material tales como la resistencia, tenacidad a la fractura, y el comportamiento a la fatiga.

Cuando una grieta crece en el llamado rango de Paris, la región II b crecimiento estable de la grieta, el mecanismo de fractura es similar a la fractura estática.

2. Introduction

2.1.Composites

A lot of modern technologies required materials with an unusual combination of properties impossible to get with metals, ceramics and polymers individually.

The concept of composite materials was put forward to break the processes of strengthening of alloy also acquire higher strength, higher stiffness, better heat resistance and greater wear resistance. This method has been applied successfully in the field of polymers; therefore, many practical materials have been developed successfully. However, we must recognize that the application of this method to MMC or ceramic matrix composites has started too late.

A composite is a material system composed of a mixture or combination of two or more micro or macro-constituents that differ in form and chemical composition and are insoluble to each other.

The design of composites has combined certain metals, ceramics and polymers to produce a new generation of special materials that have been developed to improve the rigidity, toughness and tensile strength at both room temperature and at elevated temperatures. The combinations of properties of materials have been extended through the development of composite materials, are multiphase materials obtained artificially. The constituent phases must be chemically different and separated by an interface. For this reason, most metal alloys and many ceramics do not fit in this definition, because their multiple phases are formed by natural phenomena.

Most of the composite materials are composed of two phases, a so-called matrix which is continuous and surrounds the other phase, the dispersed phase. The properties of composites are based on the properties of the constituent phases, their relative proportions and the geometry of the dispersed phases.

The main importance of a composite material for the engineering is that two or more different materials are combined to form another whose properties are superior to those of its individual components (synergy).

2.2. Components of material

2.2.1. Matrix

The functions of the matrix in a composite material are:

- Maintain the reinforcement in position work and distribute the load between them.
- Protect the reinforcement of mechanical and chemical deterioration.
- Avoid crack propagation.

Of the different classifications that we can make of composite materials, perhaps the most important is in relation with matrix and which we can identify three main groups:

A. Metal matrix composite (MMCs)

The metal matrix composites have been designed especially for structural applications in the automotive, aerospace, military, electrical and electronics, which usually require stiffness, strength and specific modulus.

The composites have high strength and low weight. The main efforts have been directed to obtaining MMCs of low density , with matrix of light alloy, among which stressed the group of materials based on aluminum, by wide range alloys, numerous possibilities of processing of heat treatment and indicted quite flexible.

In metal matrix composites is improved creep behavior on the basis alloy, being obtainable directionality properties: this increased resistance is associated with a decrease in toughness of the alloy. It is necessary special fibers to prevent chemical reaction at high temperature fiber matrix: manufacturing costs are very high and there is little experience in service behavior.

The composites are classified in three groups according to the type of reinforcement incorporated: reinforced with continuous fiber, discontinuous fibers and particles. Thus, we found as examples of the metal matrix composite aluminum alloys reinforced with boron fibers, particles of alumina, silicon carbide…

B. Ceramic matrix composite (CMCs)

These composites are newer and improved the mechanical properties such as the strength and toughness of traditional ceramic materials, especially in low temperature range. Also are classified according to the type of reinforcement incorporated: reinforced with continuous fibers, discontinuous fibers and particles.

The main fibers that are combined with ceramic matrix are silicon carbide and aluminum oxide, and in the case of discontinuous fibers and particles are used as reinforcement needles silicon carbide ceramics.

Ceramic matrix composites exhibit enormous complexity, both in behavior as in its industrial production. The objective is to have a ceramic material with the thermal resistance that have the ceramics materials, but with a tenacity value that allows their use in structural applications.

Three-dimensional fabrics graphite fiber, which infiltrates between the carbon matrix by an iterative process of pyrolysis and / or vapor phase position, have been developed for external coating of space shuttles, or disk brakes for airplanes and racing cars.

C. Polymer matrix composite (PMCs)

The polymer matrix composites, we can define as materials with good mechanical properties, corrosion resistance and chemical agents, and by their specific characteristics, can be molded with absolute freedom of forms.

We can stand out from these thermoset composites, with its main group of matrix: polyester resins, vinyl ester, epoxy and phenolic. As reinforcing materials: glass fibers, the aramid (kevlar) and carbon, in the form of numerous types of single or combined textile structures.

The choice of material that constituting the matrix depends mainly of the strength, temperature, density and cost required for the intended application. Other factors, such as ductility, fracture toughness and fatigue resistance, are more important after the metal has been selected.

One of the most important factors is the compatibility of the matrix material with the reinforcement. The compatibility, in this case, means that there is not undesirable chemical reaction at the interface of the matrix and the reinforcement. In some instances, this reaction can lead to the formation of intermetallic compound at the interface which can affect adversely the charge transfer to the backing. Also the reaction products may act as nucleation sites of cracks.

The polymer matrix composites are the best characterized and most used in the industrial. Since 1980, civil and military planes incorporate progressively these materials in its external structure, up a 40% of the total weight. It requires improve tolerance to damage, or ability of the structure to withstand the usual service accidents (corrosion, impacts, etc.), without significant degradation of their properties.

2.2.2. Reinforcements

The composites can also be classified according to the type of reinforcement. The reinforcement is the phase surrounded by the matrix material. The properties of composite materials are based on the properties of the constituent phases, their relative proportions and the geometry of the reinforcement, the shape, size, distribution and orientation. The reinforcements may take the form of particles, flakes, whiskers, short fibers, continuous fibers or sheets.

A. Continuously reinforcement materials

Reinforcements are used as continuous fibers or filaments, as well as metal wires, with these fibers are obtained more resistant materials than with any other type of reinforcement. The different types of fibers are:

- *Glass fibers*: These fibers are used to reinforce matrix plastic and to do structured compounds and molded products. The glass fiber is the most used and also has the lowest cost. Composite materials reinforced with glass fibers have the following favorable properties: good strength to weight ratio, good dimensional stability, and good resistance to heat, cold, humidity, corrosion resistance and good electrical insulating properties.

- *Boron fibers*: Boron is a brittle material. It is produced commercially by chemical deposition of boron vapor on a substrate, typically a tungsten filament, so boron fibers are a composite material.

- *Carbon fibers*: Carbon is an element very lightweight and with a low density. The elastic modulus of carbon fibers depends of the degree of perfection of the orientation, which varies considerably with the conditions and the manufacturing process. The imperfections in orientation produce complex hollow, elongated and parallel to the fiber axis, so that these points act as stress concentration points and weak points produce the reduction of the properties.

- *Organic fibers*: the concept of organic fibers is based on the creation of fibers with high strength and high modulus of elasticity from a perfect alignment of polymers. Currently, fibers of polyethylene are of high density and high modulus of elasticity, with the maximum linearity and elongation between the polymer chains during the manufacturing process, during the spinning and drawing.

- *Ceramic fibers*: This type of fibers has an attractive set of properties, combine high strength and good value of elastic modulus at high temperature, also these fibers have not suffer too much degradation due to environmental exposure. These fibers are appropriate for high temperature applications.

B. Discontinuously reinforced materials

The main advantage of these composite materials is that can be fabricated using processing techniques similar to those used to obtain the unreinforced matrix, so the production cost is lower.

These materials have relatively isotropic properties due to a lower relation of formation of reinforcement and greater random orientation thereof.

Discontinuous reinforcements consist mainly of silicon carbide (SiC) in the form of whiskers or particles, and alumina (Al_2O_3) in the form of short fibers and particles.

- *Whiskers*: Are monocrystalline acicular crystal materials which have a length to diameter ratio very high. Because of their small diameter, have a high degree of crystalline perfection and are almost free of it are flawed, for high resistance.

  Therefore, the use of composites reinforced with whisker, may provide opportunities to reduce operating costs in the life cycle of many applications of critic weight. However, have the disadvantage of not having a uniform size, therefore, varying properties.

- *Particles*: Particles can have a lot of different geometries. The reinforcement is much more effective, when the particles are small and are distributed homogeneously in the matrix. Moreover, the volume fraction of the two phases influences the behavior, the mechanical properties improve when increasing content of particles, are relatively cheap.

- *Short fiber*: have bigger form relation and are prepared with random orientation, often are used as preform for some MMC casting processes. Despite their good mechanical performance level with a relatively low cost, the nature of reinforce limits the secondary options of manufacturing of resulting material.

C. Effect of reinforcement

In the composites, mechanical properties depend on the number, size, shape and distribution of the dispersed phase, in addition to the mechanical properties of the matrix and the nature of the interface.

The advantages of composite materials compared to unreinforced materials are in general:

- High strength and stiffness
- Better behavior high temperature, showing greater strength and better creep properties, because the reinforcing element has a high melting point in general.
- Low coefficient of thermal expansion in general, depending on the reinforcement.
- Resistance to fatigue through the use of certain fibers

In short, the characteristics that make it attractive to the composite materials are:

- High specific stiffness
- High thermal conductivity, good electrical conductivity, minimum charge electrostatic
- Very low thermal expansion
- Do not absorb moisture, no problems degassing, removing or polluting byproducts
- They are able to withstand high temperatures

2.3. Composites with metal matrix

Metal matrix composites contain ceramic reinforcements in a metallic alloy matrix. The matrix may be an Al or Ti alloy, while the reinforcements may be Al_2O_3 o SiC. The reinforcements may be in the form of fibers, whiskers or particles. Particle reinforced metal matrix composites are the most economical and the most popular. These composites typically contain angular ceramic particles 1-50 μm in size and aspect ratios of 1-2, and offer higher stiffness, elevated temperature strength and wear resistance as

compared to the unreinforced metallic alloys. Some examples where are used these composites are: in the antenna waveguide mast of the Hubble space telescope, the ventral fins and fuel access covers of the F-16 fighter jet aircraft and blade sleeves of the Eurocopter, also to the automotive applications like the cylinder liners (Honda Prelude), driveshafts (Chevrolet Corvette). However, the applicability of the MMCs is limited by their low ductility, and their failure strains are almost an order of magnitude lower than that of the metallic alloys.

The MMC failure strain influenced by the intrinsic properties of the different phases (metallic matrix, the ceramic particles and the metal-ceramic interface) and certain geometrical factors such as the size , shape and spatial distribution of the ceramic reinforcements. The ductility of these materials may thus be enhanced by a suitable choice of the above variables. The greatest scope possibly lies in the modification of the metal-ceramic interface and the spatial distribution of the ceramic particles. The composite microstructure may be engineered at the primary processing (e.g. casting) stage of a conventional composite fabrication process, e.g. through choice of a proper processing route for a development of optimal interfaces. The property optimization may even occur at the secondary processing stage, e.g. through high temperature extrusion of as-cast composite samples to eliminate the casting defects and modify the reinforcement distribution.

The failure models for heterogeneous metallic systems (which include the metallic alloys and the MMCs) are relatively well developed for low second phase volume fractions. In this case, the failure mechanism comprises of three distinct steps: (a) void nucleation, generally by cracking of the reinforcements or by decohesion at the reinforcement-matrix interface, (b) void growth primarily along the loading direction, and (c) coalescence of voids to form the macro-crack. Additionally, the reinforcement distribution in commercial MMCs is non-uniform, and the local reinforcement volume fraction may be higher than the nominal volume fraction in certain regions. These high reinforcement volume fraction regions are called clusters. The reinforcement clusters have been experimentally observed to dominate the failure mechanism in commercial composite materials, and preferential initiation and propagation of damage have been

detected in these regions. The interaction between the reinforcements and the nucleated damage in the clusters is thus critical to the failure mechanism of the MMCs.

3. Fracture behavior

3.1. Modeling of composite deformation

3.1.1. Elastic analysis

The effect of the reinforcements on the mechanical behavior of the composite materials has been evaluated at different levels of complexity and precision, depending on the expressions for the division of the stress and strains in the two phases. At the simplest level, the strain or the stress may be assumed to be equal in the two phases. The strain equality (the Voigt model) appears during axial deformation of continuously reinforced composites, while the equality of the phase stress (the Reuss model) develops during transverse deformation of composite laminates. These two situations represent the upper-bound and the lower-bound respectively of estimates of the MMC deformation characteristics.

For the upper bound, the composite stress (σ_a^c) and strain (ε_a^c) in the axial direction can be written in terms of the stress and strain in the matrix (σ_a^m, ε_a^m) and reinforcement (σ_a^r, ε_a^r) and the volume fraction of the reinforcing phase (f).

$$\sigma_a^c = (1-f)\sigma_a^m + f\sigma_a^r$$

$$\varepsilon_a^c = \varepsilon_a^m = \varepsilon_a^r$$

The axial elastic stiffness (E_a^c) is:

$$E_a^c = (1-f)E_a^m + fE_a^r$$

For the lower bound:

$$\varepsilon_t^c = (1-f)\varepsilon_t^m + f\varepsilon_t^r$$

$$\sigma_t^c = \sigma_t^m = \sigma_t^r$$

And the composite transverse elastic stiffness (E_t^c) is:

$$1/E_t^c = (1-f)/E_t^m + f/E_t^r$$

The Voigt model is valid for the axial deformation of fiber reinforced composites. During transverse deformation of the fiber reinforced composites, the stresses in the two phases are generally unequal. For elastic loading, several empirical expressions have been suggested for the transverse elastic modulus.

For discontinuously reinforced MMCs, both the stresses and the strains in the two phases may be different, and the composite property predictions need to account for the complex nature of the stress/strain partitioning between the two phases. For an isolated ellipsoidal elastic reinforcement in an infinite elastic matrix, a procedure for evaluating the stresses and the strains in the two phases was developed by Eshelby [1957].

For plane strain deformation of elastic composites reinforced by cylindrical fibers, the stress/strain fields in the matrix and reinforcement were evaluated by Muskhelishvili [1953].

Direct uses of the Eshelby or Muskhelishvili models are limited to a dilute distribution of reinforcements. Brown and Stobbs[1971], Tanaka and Mori[1972] and Pedersen[1983] later extended Eshelbys approach to compute stresses in non dilute composites, by assuming that the volume averages of the internal stresses in the different phases are zero, while the volume average of the phase stresses is equal to the applied stress. These models are generally called the mean-field models. The solution of the composite stresses from such models is relatively simple to evaluate, but primarily limited to ellipsoidal reinforcements and elastic matrices. On the other hand, the MMC matrices are elasto-plastic, and the reinforcement shape in the MMCs may be arbitrary. To overcome these problems, numerical models of composite deformation (primarily finite element models) have become prevalent in recent years.

3.1.2. Elasto-plastic analysis

Drucker [1965, 1966] laid the foundation for analyzing the effects of the reinforcements on the overall stress-strain response of a composite material with an elasto-plastic matrix. He observed that for low volume fractions of rigid inclusions in a perfectly plastic matrix the effect of the inclusions on the overall composite deformation would be small (figure 3.1(a)). However, for a work-hardening matrix, the presence of the inclusions would block the slip in a number of planes, thus giving rise to matrix (figure 3.1(b)). Depending on the length scale of the model, these studies can primarily divided into two categories, the self-consistent models and the micromechanical (finite element) models.

(a)

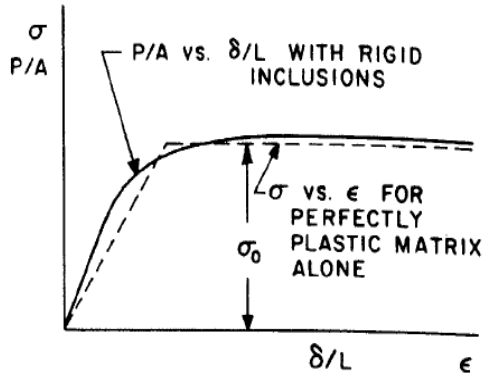

(b)

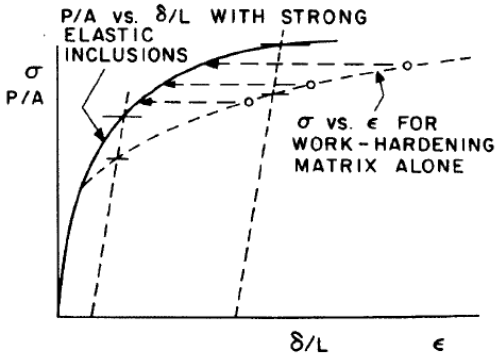

Figure 3.1 Engineering stress-strain curves for the composite and the unreinforced matrix, for (a) completely plastic matrix and (b) work-hardening matrix [Drucker, 1966].

A. Self -consistent (mean field) models

The self-consistent models are similar to the mean-field models, and compute the average (or mean) stresses in the reinforcing phase and the matrix. They treat phases as if are embedded in an infinite medium (effective composite), and determine their deformation characteristics by the Eshelby method. The stress in the reinforcements (σ^p) and the matrix (σ^m) are given by [Corbin and Wilkinson, 1994].

$$\sigma^p = C_p\big(SC_p + (1-S)C_c\big)^{-1}\sigma^A$$
$$\sigma^m = C_m(SC_m + (1-S)C_c)^{-1}\sigma^A$$

Where C_p, C_m and C_c are the stiffness of the reinforcement, matrix and composite respectively, S is the Eshelby tensor and σ^A is the applied stress. The matrix and the reinforcement stiffness are represented by their Young's moduli for elastic and by their tangent [Corbin and Wilkinson, 1994] or the secant moduli for plastic deformation [Wilkinson, 1997]. Corbin and Wilkinson observed that the initial work-hardening rate and the flow stress of the composite were higher than that of the unreinforced matrix. This strengthening effect of the reinforcement increased with increase in the rate of matrix work-hardening.

The above analysis assumes a uniform distribution of the reinforcements. However, it can be modified to account for the non-uniformity of reinforcement distribution, by dividing the composite into reinforcement-depleted and high reinforcement density region (or reinforcement clusters). The properties of these two phases or regions may then replace the properties of the matrix and the reinforcement respectively in the analysis above. Corbin and Wilkinson observed that non-uniformity in reinforcement distribution enhanced the initial work-hardening rate and the flow stress in the composite. The maximum enhancement was achieved when approximately one-half of all the reinforcements are in clusters.

These models do not explicitly account for the interactions between the stress-strain fields of the reinforcements. The self-consistent models are generally suited to modeling composite deformation at relatively large length scales, e.g. prediction of the macroscopic stress-strain behavior or the average stress in the different phases.

B. Micromechanical (Finite element) models

Finite element models are well suited for modeling of local stress/strain fields for composite deformation processes. The method involves discretizing the continuum into a finite number of elements, whose deformation may be characterized in terms of a finite number of parameters. Each element is assigned material properties characteristic of the bulk properties of either the matrix or reinforcement phase (or any other phase present), depending on which phase the element represents. The finite element solution involves finding a displacement-force field which minimizes the total energy of the domain, subject to the given boundary conditions and the material constitutive models, such that the equilibrium of the forces and the compatibility of the displacements are maintained for all the elements.

The effects of the reinforcement shape or volume fraction on composite deformation has been extensively studied using finite element models.

Bao [1991] has studied the effect of reinforcement volume fraction and shape on the composite flow stress. They observed that the ceramic particle enhanced the initial work-hardening rate of the composite. However, for both perfectly plastic and strain hardening matrices, the composite work hardening rate was similar to that of the unreinforced matrix beyond a strain> 10 times the yield strain. The enhancement of the initial work hardening rate was higher for reinforcements with higher aspect ratios and angularity. Cylindrical reinforcements (under axial loading) were more effective than ellipsoidal (with similar aspect ratio) or spherical reinforcement for composite strengthening. The strengthening effect also increased for higher reinforcement volume fractions. Levy and Papazian [1990], simulating the tensile deformation of AA5456-SiC_w composites also observed increased composite strengthening effects of reinforcements of various shapes, including whiskers (aspect ratio=5), unit cylinders, truncated cylinders, spheres and double cones, for a Al-3.5%Cu-20% SiC composite.

The predicted composite stress-strain diagrams for the different reinforcements are shown in Figure 3.2(a). It can be seen that the high aspect ratio whiskers can provide the highest strengthening, while the double conical shape was the least effective reinforcement. Figure 3.2(b) shows the computed hydrostatic stress levels in the matrix for the different reinforcements. The hydrostatic stress distributions correlate with the composite stress levels shown in figure 3.2(a).

(a)

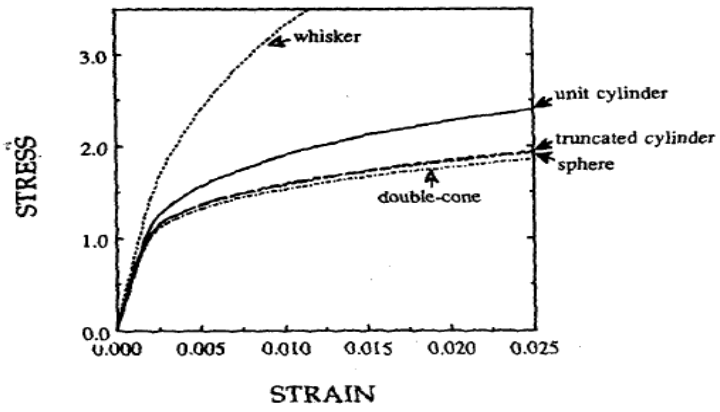

(b)

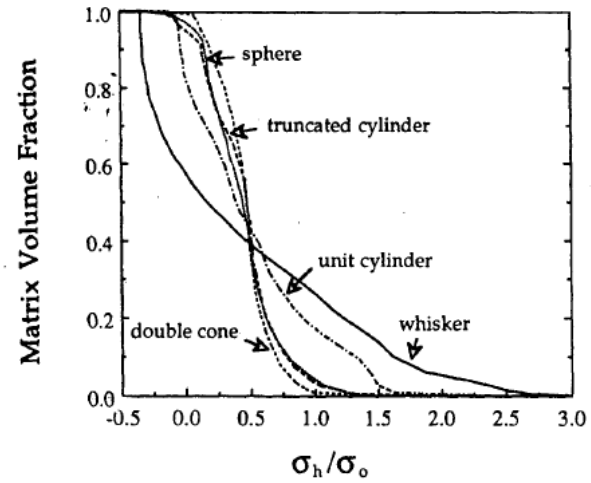

Figure 3.2 (a) Composite flow stress for different reinforcement shapes, and (b) the corresponding distribution of matrix hydrostatic stress for a Al-Cu-20% SiC reinforced MMC [Shen (1995)].

The effects of reinforcement distribution on the composite strengthening have also been extensively studied. Generally, the reinforcement arrangements analyzed were periodic and were either square-edge, square-diagonal or triangular (figure 3.3). At low or moderate reinforcement volume fractions, the square-edge packing of the reinforcements was observed to lead to maximum composite strengthening [Christman (1989), Brokenbrough (1991), Nakamura and Suresh (1993), Zahl (1994), Poole (1994)]. Christman [1989] modeled the strengthening effects in a AA2124-13.2%SiCw composite for a square-edge reinforcement arrangement (uniform distribution) and arrangements in which the reinforcements were shifted horizontally and vertically (figure 3.4). They observed that any deviation from the square-edge arrangement lowered the hydrostatic stress levels arising due to constrained matrix flow, and decreased the composite flow stress. The effect increased with the degree of shift from the square-edge arrangement and was higher for the vertical shift than the horizontal one.

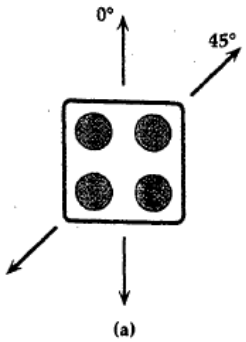

Figure 3.3 The square-edge (0º orientation in (a)), square-diagonal (45º orientation in (a)) and triangular arrangement (b) of reinforcements [Zahl, 1994].

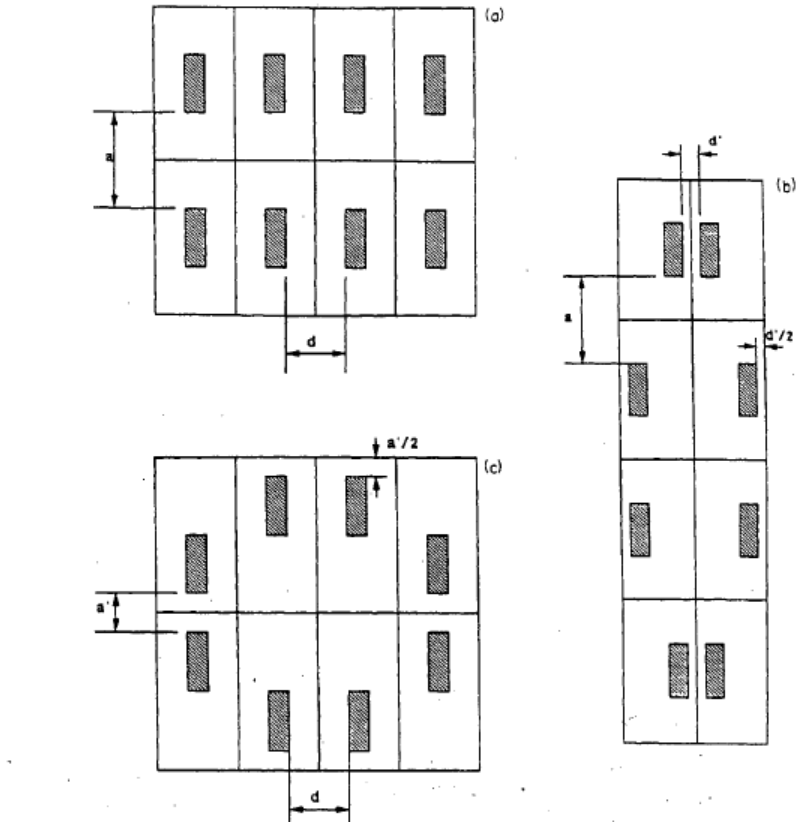

Figure 3.4 (a) square-edge arrangement, and arrangements involving (b) horizontal shift and (c) vertical shift [Christman,1989].

Brockenbrough studied the strengthening characteristics of a continuously reinforced AA6061-46%B (cylindrical fibers) MMC for various uniform fiber arrangements (square-edge, square diagonal and triangular) as well as for a random arrangement of 30 fibers. They observed that the axial deformation characteristics of the composites were independent of the fiber arrangements. However, the composite stress-strain diagrams for both transverse tensile and transverse shear deformations varied with the fiber arrangements (figure 3.5).

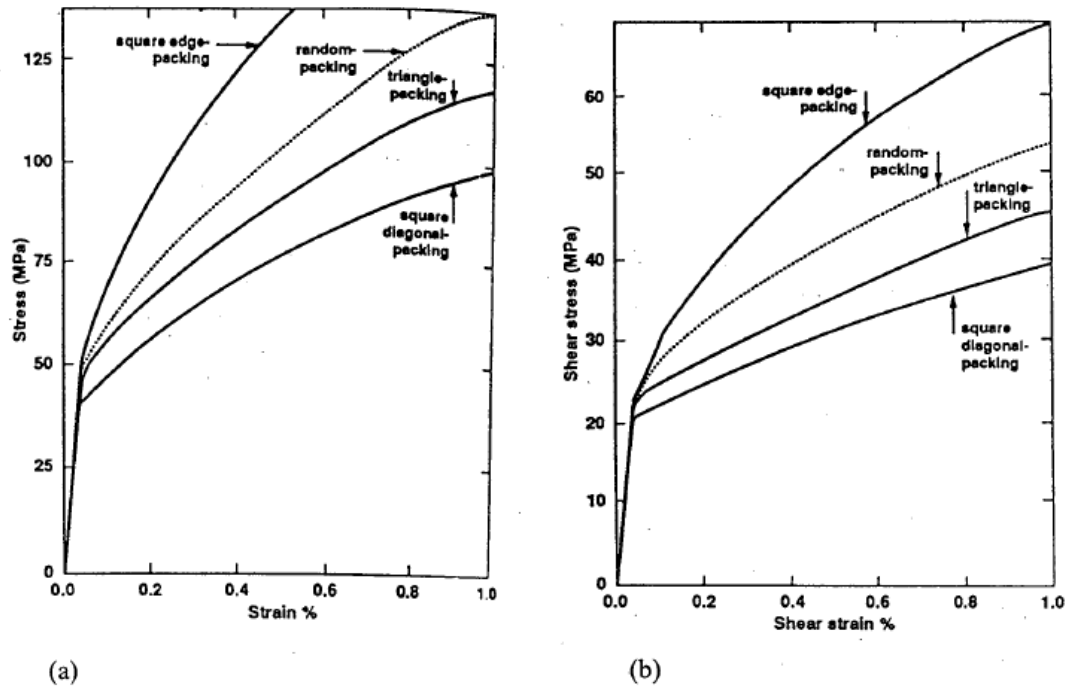

Figure 3.5 The effect of reinforcement arrangement on the composite flow stress under (a) transverse tensile and (b) transverse shear deformation [Brockenbrough,1991].

The effect of the reinforcement arrangement on the local stress/strain fields in the reinforcement and matrix has been studied by Brockenbrough [1992], Tvergaard [1995], Watt [1996], Ghosh [1997] and Axelesen and Pyrz [1997]. Brockenbrough simulated the deformation of a Al 10% Si composite using real microstructural geometry (i.e the actual positions and sizes of the particles were incorporated in the model, although their shapes were changed to circular cross sections). They observed that intense plastic strains developed around the larger particles, and the maximum reinforcement stress was observed in particle clusters (where the particles were very close to each other). Experimental and numerical studies by Poole [1994] compared the local stress/strains developed during transverse deformation of a Cu-W continuously reinforced composite (20% and 30% fiber volume fraction) for a square-edge and triangular fiber packing. They observed the matrix strain concentrations occurred in between the fibers along the loading direction for a square-edge packing, and perpendicular to the loading direction for the triangular packing of the fibers. The maximum reinforcement stress (principal stress along the loading direction) was significantly higher for the square-edge packing,

as compared to the triangular arrangement. Tvergaard [1995] also observed that the high reinforcement stresses correspond to a square reinforcement arrangement. Watt [1996] numerically computed the local stress fields for AA6061 SiC composites for a square-edge reinforcement distribution and that for distributions with smaller inter-particle spacing along or perpendicular to the loading direction. They observed that decreasing the inter-particle spacing along the loading direction significantly enhanced the hydrostatic stress and the maximum principal stress in both the reinforcements and the intervening matrix in the loading direction. Ghosh [1997] used a novel Voronoy cell based finite element method to simulate the deformation of various composite microstructures, reinforced to different volume fractions and with various degrees of clustering. Axelsen and Pyrz [1997] simulated the deformation of an elastic matrix-elastic reinforcement composite for a random and a completely clustered (i.e. all the reinforcements lied in clusters) microstructure. They observed higher radial stress at the reinforcement interface for the clustered microstructure.

3.2. Formation of microdamage caused by deformation

The breakage of the MMC occurs by a process of nucleation, growth and coalescence of voids (Van Stone 1985). The nucleation of cavities in the material can occur by breaking ductile of the matrix, decohesion of the matrix-reinforcement interface or breakage brittle ceramic reinforcement (Llorca 1991, Lloyd 1991, Needieman 1993 and Derby 1993 and 1995).

3.2.1. Void formation in the matrix

The ductile fracture of the matrix is the failure mechanism observed in MMC based alloys where appear intermetallic with a size of the order of several microns. These phases are normally due to the presence of impurities such as iron in the matrix composition and are preferential sites for nucleation cavities. The presence of other particles in the lower size in the microstructure of the matrix, as precipitates or

dispersions hardeners, promotes the nucleation of cavities around larger phases and their subsequent growth and coalescence. The growth of nucleated voids in the matrix is promoted by the constraints imposed by the ceramic reinforcement which increases the hydrostatic stress (Llorca 1991 and 1993 Needieman).

The next figure 3.6 shows the result of SiC whisker reinforced 6061 aluminum alloy obtained through an analysis by elastic-plastic finite element method, which demonstrates distribution of stress and strain in the matrix when a tensile stress is loaded in the direction parallel with reinforcement.

In the figure 3.6 (a) we observed that the effective stress, σ_{eff}[1] concentrates around the end of whisker reinforcement, and decreases at the side. This is due to the strong restraint of elastic deformation and plastic flowing of matrix at the ends of reinforcements. The figure 3.6(c) shown a large amount of plastic deformation has occurred locally around the whisker end. Figure 3.6 (b) shows the remarkable increasing triaxial stress in matrix caused by restraint of deformation.

Accordingly, it is reasonable to believe that the increase in triaxial stress can be a reinforcing mechanism in MMC, with which it is possible for the matrix to undergo a large amount of axial stress without remarkable plastic deformation (Kobayashi 2004).

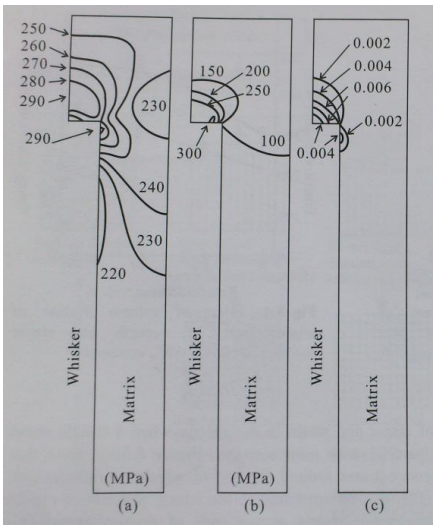

Figure 3.6 Results of FEM analysis on (a) effective stress, (b) hydrostatic pressure stress, and (c) effective plastic strain distribution in the matrix of 6061 Al-SiC composite (1/4 model, applied stress 300 MPa)[Kobayashi 2004].

On the other hand, void nucleation speed, f, can be illustrated with Eq (3.1) when the nucleation mechanism is a stress-controlled type, or with Eq (3.2) when it is a plastic strain-controlled type.

$$f = B\left(\sigma_m + {}^{\sigma_h}/_{3}\right) \quad \textbf{[Eq. 3.1]}$$

$$f = D\varepsilon_m^p \quad \textbf{[Eq. 3.2]}$$

$$B = f_N exp\left[-{}^{1}/_{2}\left\{\left(\sigma_m + {}^{\sigma_h}/_{3} - \sigma_N\right)/_{S_N}\right\}^2\right]/S_N(2\pi)^{1/2}$$

$$D = f_N exp\left[-{}^{1}/_{2}\left\{\left(\varepsilon_m^p - \varepsilon_N\right)/_{S_N}\right\}^2\right]/S_N(2\pi)^{1/2}$$

In those equations, σ_m is a flow stress, σ_h is hydrostatic pressure, ε_m^p is effective plastic strain, and f_N is particle volume fraction of the void nucleus. In addition, σ_N and ε_N are the average standard stress and strain for void nucleation, respectively, whereas S_N is the standard deviation.

In the case of the stress-controlled mechanism, growth speed decreases after nucleation because hydrostatic stress can be relieved by a large amount of void nucleation.

On the other hand, in the case of plastic strain-controlled type, initiation of damage will be delayed until the localized plastic flow develops fully because the void nucleation is limited to within constrained plastic flow range. As an analysis result shown in fig 3.7, compared with the stress-controlled case, both strength and ductility are improved more than 30% (Kobayashi 2004).

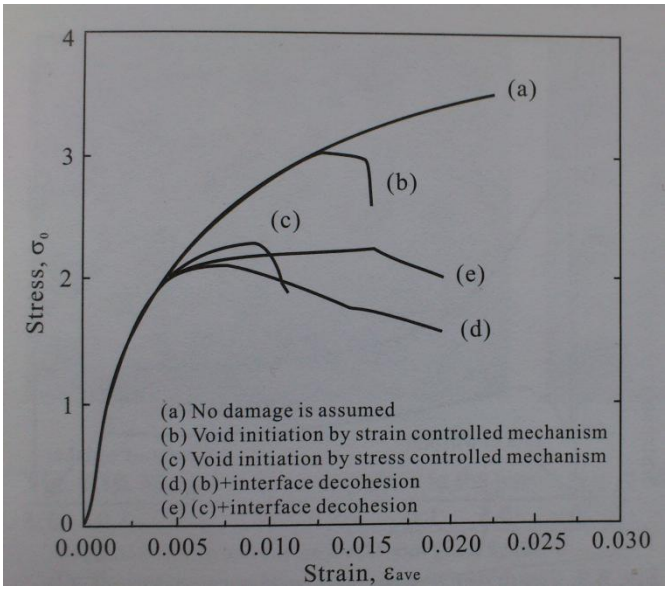

Figure 3.7 Effect of void initiation mechanism on stress-strain curve of whisker-reinforced MMC [Kobayashi 2004].

3.2.2. Fracture of Reinforcement

The failure mechanism observed in materials normally is the brittle fracture of ceramic reinforcement (Lloyd 1991, Singh 1993, Llorca 1993 and 1994). The stresses acting on the reinforcement during material deformation can exceed the mechanical resistance of the ceramic particles, resulting in brittle fracture of reinforcement before appearing cavities in the interface matrix-reinforcement (Lloyd 1991, Singh 1993, Llorca 1993 and 1994).

The larger particles are broken more frequently than those smaller; because by increasing the size particle inside major defects appear reduce mechanical resistance (Lloyd 1991 and 1993 Llorca). Consequently, by reducing the size of the reinforcement the stresses acting on the reinforcement may be insufficient to cause its brittle fracture and failure mechanism observed in particulate reinforced materials is the small size of the interfacial decohesion matrix-reinforcement (Derby 1995).

The cracking of the hard and brittle ceramic reinforcements generally occur when the maximum principal stress in the particles is higher than their strength. The reinforcement strength or the fracture stress (σ_f) is governed by the size of the largest flaw (c) in the reinforcement, where E is the Young's modulus of the particle, γ the fracture surface energy and A is a constant.

$$\sigma_f = A\sqrt{\frac{2E\gamma}{c\pi}}$$

The size of flaw depends of the size of the particle. Generally, this dependence is modeled in terms of the Weibull modulus (m) and the probability of fracture of a particle (P_{fr}) is given by

$$P_{fr} = 1 - exp\left[-\left({}^{V}/_{V_0}\right)\left({}^{\sigma_p}/_{\sigma_0}\right)^{m}\right] \qquad \textbf{[Eq.3.3]}$$

where σ_p and V are the stress in the particle and the particle volume respectively, and V_0 and σ_0 are reference volume and stress (constant for a particular reinforcing phase). So, the probability of fracture of a particle increases with increase in particle size. Moreover, since the particle stress increases with the aspect ratio and angularity of a particle, the probability of particle fracture is expected to increase for particles with higher aspect ratio and angularity. Equation 3.3 determines the probability of particle fracture for a particle population characterized by a single particle volume and particle stress (or particle aspect ratio and angularity) .On the other hand, the reinforcement shape and size in a metal matrix composite sample varies.

In the Figure 3.8 we observe the result of the same analysis as for the result in Fig 3.6, indicating axial stress distribution, σ_z, along the loading direction inside the reinforcement.

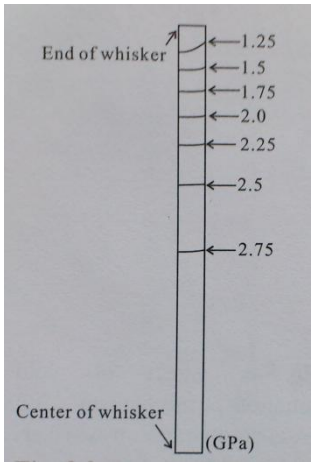

Figure 3.8. Result of FEM analysis on axial stress distribution within whisker of whisker reinforced MMC (1/4 model, tensile applied stress 400 MPa) [Kobayashi 2004].

The fracture will occur when σ_z increases over the fracture strength with interior defects of reinforcement is assumed to be SiC whiskers; in addition, it is projected that fracture of fiber does not occur at this stage because fracture strength of SiC is inferred to be higher than 8.4 GPa (Kobayashi 2004).

3.2.3. Interface Debonding

The decohesion of the matrix-reinforcement interface is the mechanism of rupture usually observed in MMC reinforced with whiskers. The ends of the Whiskers act as stress concentrators and plastic deformations are high hydrostatic tensions and facilitate the formation of cavities at the ends of the whiskers (Christman 1989 and Needíeman 1993). This failure mechanism is also observed in composites reinforced with small particle size (Derby 1995) and particle-reinforced MMC and tested at high temperature (Zhao 1994 and Poza 1996). The decohesion of reinforcement is also influenced by precipitation processes in the material. The appearance of stable phases at the matrix-reinforcement interface promotes the nucleation of voids at the ends of the reinforcement.

The interface debonding occurs when the local shear stress τ interface or the vertical stress exceeds the strength of the interface area. Figure 3.9 shows an example of an analysis result of stress distribution in the reinforcement similar to that shown in Figure 3.6 where the maximum value is approximately 150 MPa. However, the lower limit strength aluminum interfaces SiC / 6061 is reported to be higher than 1690 MPa: actually expected to be about 3000 MPa. Therefore, it is difficult to believe that the simple interface debonding occurs in this series made.

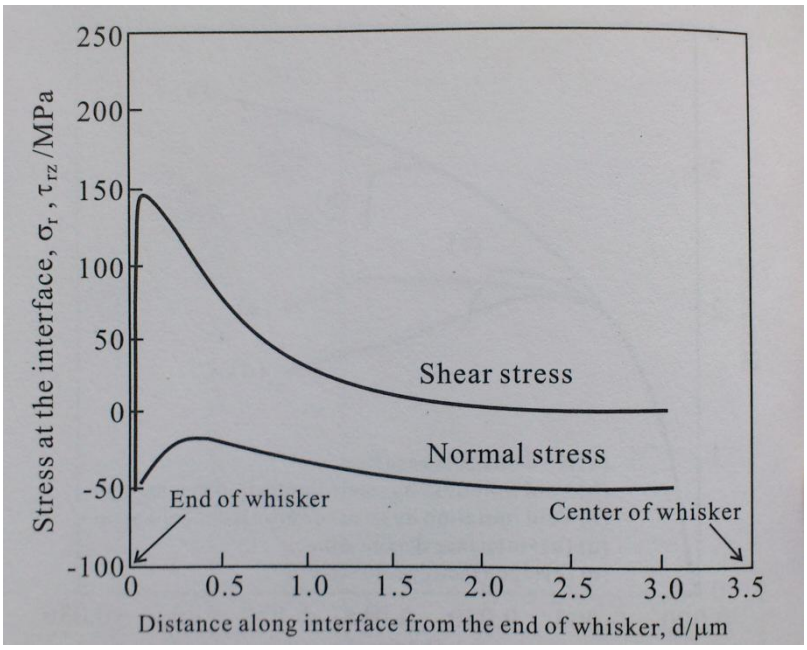

Figure 3.9 Result of FEM analysis on shear and normal stress at the whisker surface of whisker reinforced MMC (applied tensile stress, 300MPa) [Kobayashi 2004].

3.3. Fracture Process

Fracture process (damage evolution and coalescence).

If the void nucleation is sufficiently far-apart such that interactions of the stress-strain perturbation fields due to the voids and the reinforcements is insignificant, the damage evolution process for each void will be fairly independent of the others and can be differentiated into two distinct stages (a) void growth and (b) void coalescence. The stress-free surface of the voids causes strain concentrations in the adjoining matrix, and the voids grow in the loading direction at a rate which is higher than the far-field strain rate.

Fig 3.10 shows the void growth at different imposed strains for various hydrostatic stressed (σ_m) for a uniaxial tensile deformation of a non-hardening (figure 3.10). The figure shows that the void growth rate in the loading direction (a) exceeds that of the far-field strain rate (3.10). For both the non-hardening and the linear –hardening material, the void length at a strain of 0.5 is more than twice that of the original length. The void dilation rate (along the loading direction) increases with increasing hydrostatic stress and is higher for the non-hardening matrix than that for the linear-hardening matrix. On the other hand, the void shrinks along directions which are perpendicular to the loading direction.

(a)

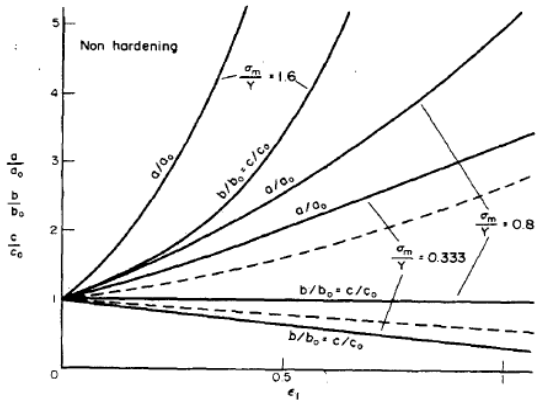

(b)

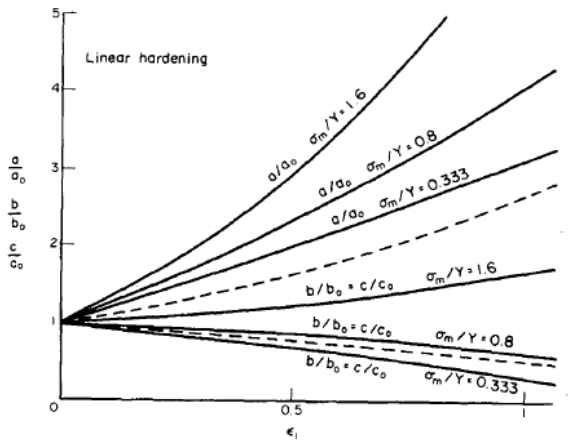

Figure 3.10 The effect of increasing plastic strain ε_1 on the principal radii (a,b,c) of an originally spherical void ($a_0=b_0=c_0$) in uniaxial tensile loading at various hydrostatic stresses (σ_m/ Y, Y is the yield strength for (a) non-hardening and (b) linear hardening material. The far-field loading is along the a-axis. The dotted lines show the changes in void dimensions as per the far-field strain field [Thomason, 1990].

The second and last stage of the void evolution process is the coalescence of the voids to form a macro-crack. During this stage, there are significant interactions between the strain concentration fields around the voids, leading to the failure of the intervening matrix and the joining of the voids. A two-dimensional criterion for the onset of void coalescence was developed by Brown and Embury [1973]. They showed that for aperiodic arrangement of voids, when the void size is equal to the inter-void spacing, 45 degree lines can be drawn between adjacent void tips (Figure 3.11(a)) and the intervening matrix will fail by shear. However, it is difficult to extend the analysis directly to the three-dimensions, since a column of material remains between voids whose lengths are equal to their spacing (Figure 3.11(b)). An alternative criterion for void coalescence was developed by Thomason [1985], who suggested that coalescence results from the attainment of the limit load in the inter-void matrix. Pardoen [1998] have conducted experimental and numerical studies on failure of notched tensile Cu bars to verify the various coalescence models. They observed that the Brown and

Embury criterion works well for low stress triaxiality. The Thomason criterion was observed to satisfactorily model the coalescence of spherical voids.

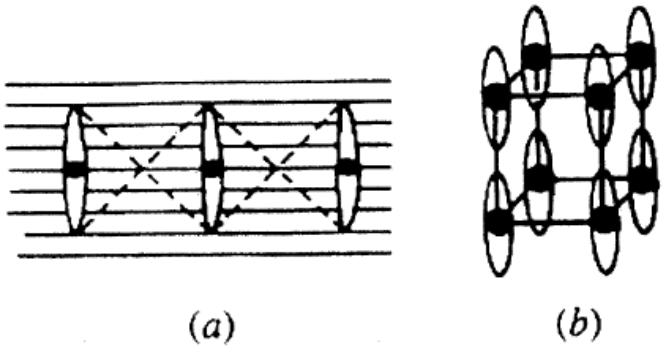

Figure 3.11 (a) Two void coalescence by Brown and Embury criterion, when void length is equal to the inter-void spacing. (b) In three dimensions, however, a column of material remains in between the voids whose lengths are equal to their spacings [Garber, 1981].

Void and reinforcement interactions

The above models can adequately describe damage evolution and coalescence process in composites with particle volume fractions typically less than 5-10%. However, when the reinforcement volume fraction is relatively high, the interactions between the stress/strain perturbation fields of the voids and the reinforcements need to be considered. The nucleation of a void warrants a reorientation of the local stress/strain fields around the damage: the damaged particle can no longer carry the previous load and the extra load has to be redistributed among the neighboring intact particles and the matrix. Work in this field has been primarily restricted to the axial loading of continuous composites, and two approximate rules have been defined (a) the global load sharing mechanism (GLS) and (b) the local load sharing mechanism (LLS). In GLS, the failure of a single fiber does not cause significant stress concentrations in the neighboring fibers, and the failure of each fiber is independent of that of another. On the other hand, LLS is characterized by the high stress concentration due to a broken fiber which leads to early failure of the neighboring fibers.

Figure 3.12 shows the expected patterns of fiber failure for both the global and the local load sharing conditions. Due to the localized nature of the failure process, the tensile strength and the ductility of the composites will be lower in the LLS regime.

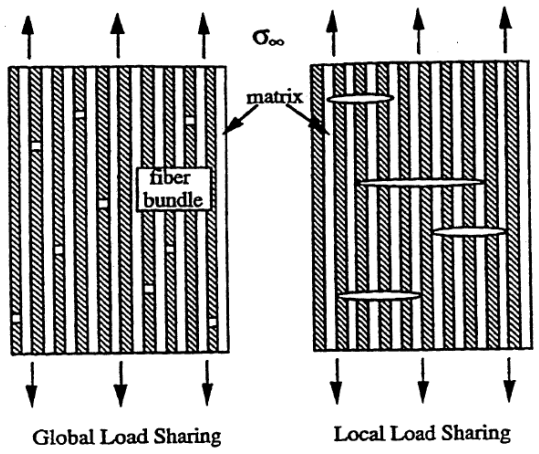

Figure 3.12 Schematic representation of fiber failure under different load sharing conditions [He, 1996].

Moreover, the figure 3.13 shows scanning electron micrographs of microscopic fracture surface of a SiC whisker reinforced alloy 6061 after the tensile test. The result shows that for the majority of patients (over 70%) enhancement was observed only in one side portion of the dimple. This result suggests that the nucleation and growth of void/coalescence near the edge of the reinforcing part in the array is the main failure mechanism in this case.

In general, the fracture of whisker reinforced MMC is controlled by void nucleation and an increase in the strain, $\varepsilon_{N,}$ where in the void nucleation to occur beginning directly improve the ductility of the material. Moreover, in particle reinforced MMC when the volume fraction of reinforcement fn that become empty cores (Figure 3.14) is low, it is in a hollow type of controlled growth. When f_N travels approximately 0.05 to 0.1, becomes a hollow type of controlled nucleation and greatly decreases ductility. Moreover, the fracture growth is controlled by a zero when f_N is low.

Rice performed an analysis for a globular hole originating from a rigid-plastic body that can be expressed as:

$$dR_V/R_V = 0.28d\varepsilon_m^p exp\left(1.5\sigma/\sigma_{eff}\right) \qquad \textbf{[Eq. 3.4]}$$

Where R_V is the void radius, σ is mean stress, and σ_{eff} is effective stress.

From Eq.3.4, equiv, it is evident that a void fraction increases rapidly as the voltage increases traction of triaxial stress. Thus the ductility decreases in a case of vacuum type controlled growth.

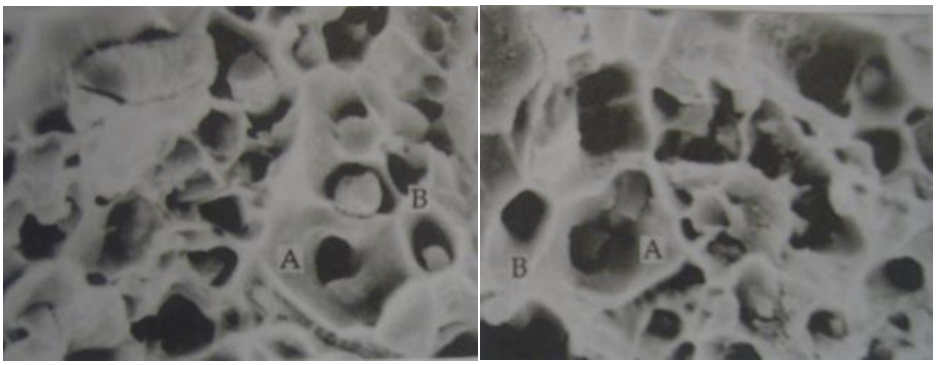

Figure 3.13 Matching fracture surface in the tensile test of 6061 Al-22% SiC_w composite [Kobayashi 2004].

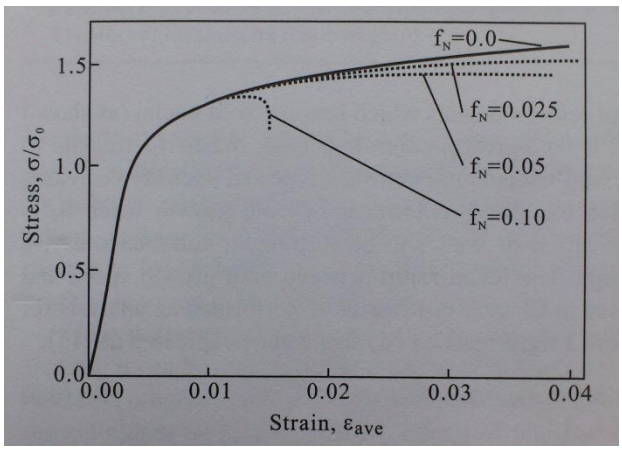

Figure 3.14 Effect of volume fraction f_N of particles which become nuclei for void formation on stress-strain curve in 2124Al-12.5% SiCp composite [Kobayashi 2004].

3.4. Crack Growth Mode under Monotonic Loading

The presence of the ceramic reinforcement in the MMC modifies its behavior mechanical increasing the resistance and reducing the ductility. When a crack propagates in MMC, damage occurs in the stress field ahead of the tip of a propagating main crack.

Figure 3.15 shows SEM examination results of fracture surface profile for 10% SiC particle reinforced 6061 alloy, where damage such as the reinforcement breakage or interface debonding can be observed within the range of 170-180 µm in a vertical direction from the fracture surface. The scale of such a damage zone differs for different materials: for the same 6061 matrix reinforced with 30% SiC, it is about 60 µm, and for 2014 alloy reinforced with Al_2O_3 particle, it is about 120 µm, moreover, for 15% SiC whisker reinforced 6061 alloy, the damage zone in front of a crack is reported to be within 30 µm [Kobayashi 2004].

Figure 3.15 Microcracks observed at fracture profile in the fracture toughness test of 6061 Al-10% SiC_p composite [Kobayashi 2004].

When the focus is limited on the aluminum alloy matrix DRM, effects of physical factors on each characteristic can be summarized in table 3.1.

Crack initiation resistance: **1) Deformation near crack tip (blunting, opening)** **2) Deflection angle before crack extension (i.e. fatigue crack extension characteristic)** **3) Stress shielding by reinforcement and microcracks initiated before crack extension**
Crack propagation resistance: **1) Stress shielding by microcracks** **2) Stress shielding by reinforcement** **3) Change of stress singularity with crack extension** **4) Crack deflection induced by crack extension driving force based on mixed mode 1) and 2) mechanisms** **5) Change of stress singularity of main crack crossing another interface** **6) Effect of secondary plastic zone in the periphery of reinforcement** **7) Effect of bridging by reinforcement**

Table 3.1 Typical factors dominating fracture toughness of particulate or short fiber reinforced MMC_S [Kobayashi 2004].

Figure 3.16 shows a schematic summary of a general crack growth model for aluminum alloy matrix DRM. As the stress shielding effect by microcrack or reinforcements, the mixed mode crack growth driving force forms, which leads to propagation of main crack toward fatal damage n front and zigzag with absorbing one after another. For this kind of material the more remarkable this crack deflection tendency is, the higher the crack propagation resistance is available.

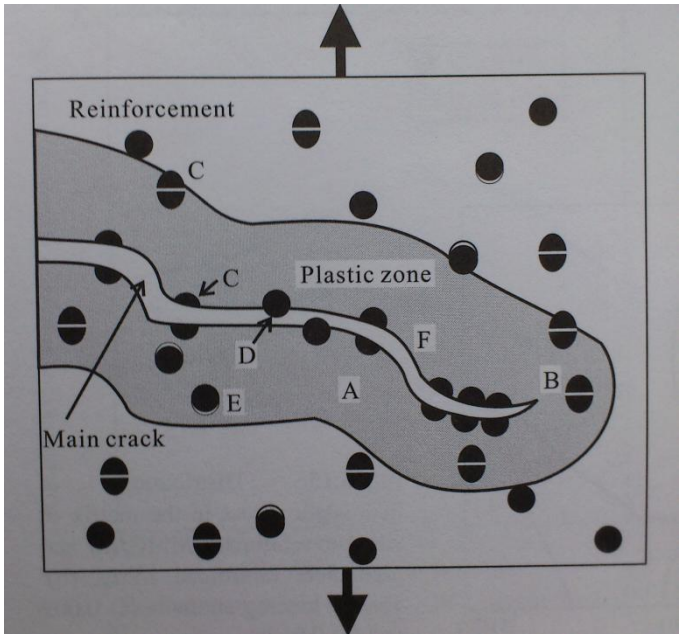

Figure 3.16 Various aspects observed during crack propagation in particulate or short fiber reinforced MMC. A: deformation in plastic zone, B: change of stress singularity with crack extension, C: rupture of reinforcement, D: stress concentration at the end of reinforcement, E: decohesion and microcrack formation, F: deflection of main crack along the path of microcracks.

3.4.1. Elastic deformation

The Young's modulus always increases due to the presence of the ceramic reinforcement, and this increase is a function of the volume fraction of ceramic particles.

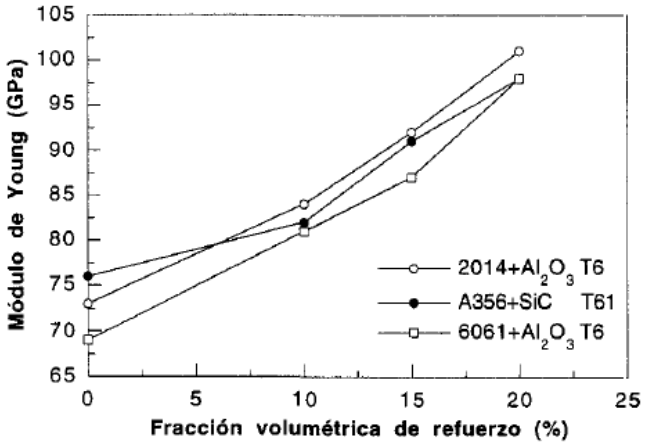

Figure 3.17 Variation of Young's modulus as a function of the content of reinforcement [Lloyd 1994].

The improvement of Young's modulus is produced by transferring of load of the matrix to the ceramic particles due to the increased stiffness of these. To produce the transfer of load of the matrix to the reinforcements is necessary that the interface particle-matrix has a good mechanical strength.

The factors controlling the increase of Young's modulus are volume fraction of reinforcement and shape of the ceramic particles. The higher the content of reinforcement the greater the burden on the ceramic particles and therefore the higher the Young's modulus. The transfer of load of the matrix to reinforcement is more effective the more elongated are the ceramics particles. As a result the increase of elastic modulus is greater for elongated reinforcements, such as whiskers, that for particles with a form factor near unity. As in alloy conventional aluminum, the Young's modulus of the compounds is not modified by heat treatments.

3.4.2. Plastic deformation

Unlike the elastic behavior, controlled mainly by the characteristics of the reinforcement, the plastic deformation of the MMC is strongly influenced by the properties of the matrix. The different alloying elements in the matrix, as well as the heat treatments are determinants factor the yield strength and tensile strength of the compounds. The mechanical strength of the MMC, increases relative to measure

unreinforced alloys, although the increase in the elastic limit is reduced by increasing the strength of the matrix (Figure 3.18).

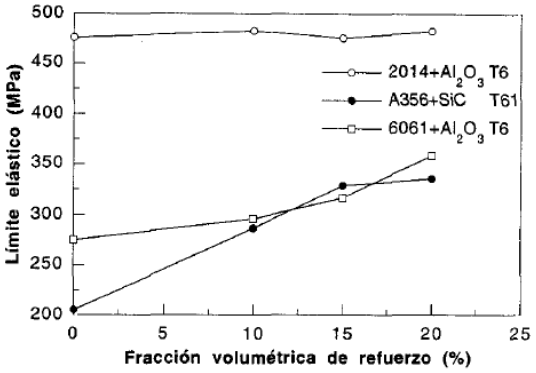

Figure 3.18 Variation of yield with the reinforcement content [Lloyd 1994].

The hardening of the MMC produced by the presence of reinforcement is due to different mechanism that can be separated in two groups: those related to the micro-structural changes induced in the matrix by the presence of the particles and those associated with the load transfer of the matrix to the reinforcements (Derby 1988, Miller 1990, 1991, Wu 1992, Lloyd 1994).

From a viewpoint microstructural the three mechanisms must be considered in the MMC hardening. The hardening of Orowan caused by the same ceramic particles, the hardening caused by the generation of dislocations in the particle-matrix interface, and hardening grain size reduction (Miller 1990 1991 and Wu 1992).

The hardening of Orowan is caused by the resistence that the ceramic particles provide the step of dislocations.

3.5. Microstructure

3.5.1. Microstructural factor of reinforcement

Factors reinforcement microstructural.

The parameters which characterize the microstructures of the reinforcement from the viewpoint of its mechanical behavior are:

- The characteristics of the population of particles (volume fraction, shape, size, slenderness, and orientation of reinforcement particles.

- The spatial distribution of the reinforcement (uniformity or presence of groupings or clusters of particles).

The volume fraction of ceramic particles improves the Young's modulus and yield strength of the composite but decreases the ductility. The shape of the particles influences in its mechanical behavior in terms of the intensity of the effect of stress and strain in zones in the matrix near the reinforcing particles, this concentration is softer in the case of spheroidal particles and more intense if the particles have irregular shape with edges.

The spatial distribution of the particle of reinforcement in the matrix, can affect in some of the mechanical properties of the compound (yield strength, ductility...) as in the localization process of deformation and damage during mechanical stress. In some cases, the particles are not evenly distributed in the matrix; the different factors affecting the final distribution of the reinforcement are the mixing process, gravity segregation before of the solidification and the expulsion of the solid-liquid interphase and segregation to the interdendritic region which solidified later. As result occur orderings of the particles or the occurrence of clusters (clustering), as seen in figure 3.19 the trend depending mainly solidification speed.

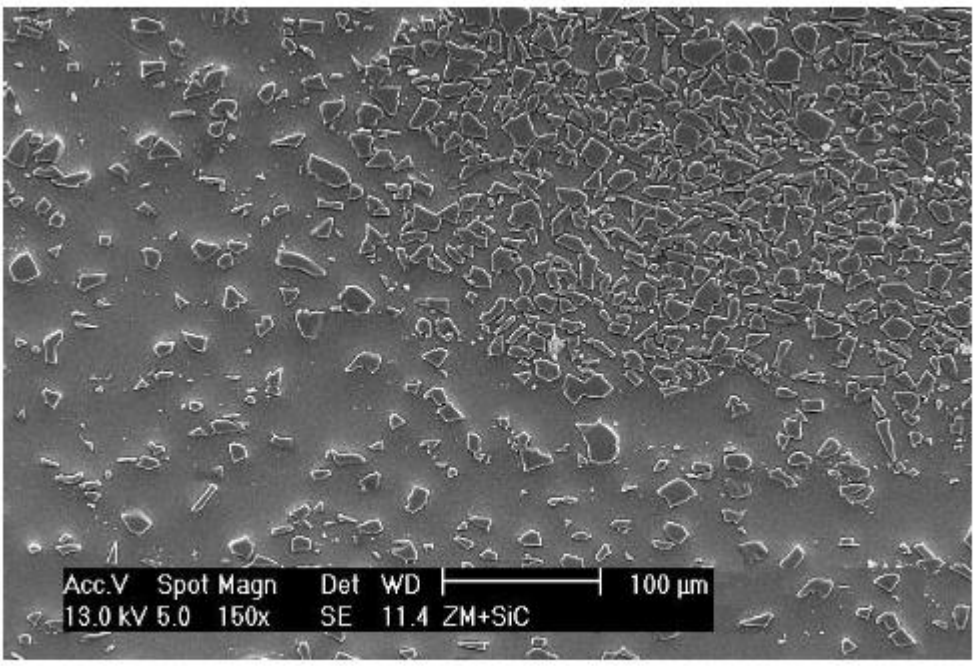

Figure 3.19 Cluster or groups of particles.

Furthermore, the composites are aged after manufacture by heat treatment which leads to recrystallization of the material. The presence of particle favors the onset of recrystallization nuclei, however, if the particles are close together prevent grain growth and recrystallization may not occur.

First, the reinforcement shape can be expressed with two parameters: the aspect ratio and shape of the end part.

It has also been reported that, though the residual strain after plastic deformation increases with increasing aspect ratio, there is no so strong influence on the residual strain, which is caused by the difference in the thermal expansion coefficient between the reinforcement and matrix. For example, compared with a globular particle reinforced composite, there are several times higher hydrostatic stress and higher stress concentration in the vicinity of reinforcement in whisker-reinforced composite, as shown in fig 3.20. Furthermore, it has been reported that though there is no evident difference in strength and elastic modulus between a cylindrical shape and a globular

shape reinforcement, the rupture strain of the globular-shape reinforcement is about 40% higher than that of a cylindrical shape [Kobayashi 2004].

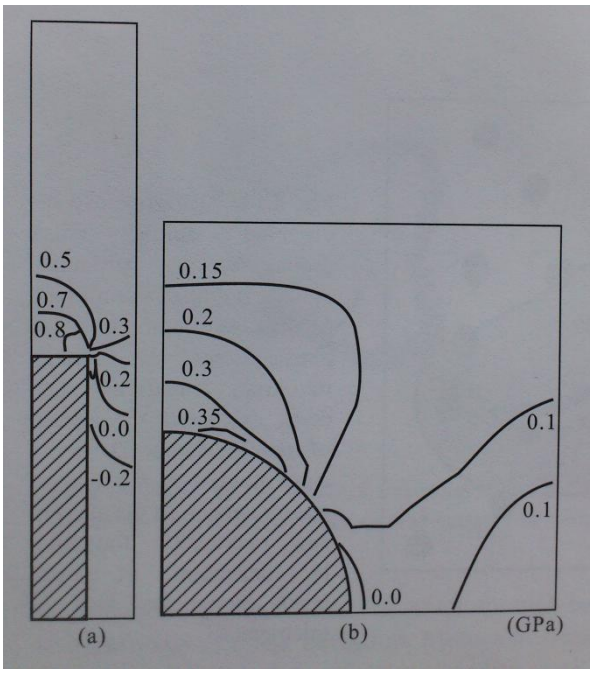

Figure 3.20 Distibution of hydrostatic stress in the matrix of whisker reinforced MMC (a) and particulate reinforced MMC (b). Tensile loading strain is (a) 0.009 and (b) 0.0108 [Kobayashi 2004].

Second, we address the size effect. It has been reported that when SiC particle size is changed from 3µm to 30µm as reinforcement for A1070 alloy or A5050 alloy, the damage mechanism of the composite changes from the interface debonding to the particle breacking. Embury pointed out that for A356 alloy reinforced with SiC particles with an average diameter of 12.6µm, the particle breaking probability for particles of diameter of 10-15µm are relatively low, while for particle diameters of more than 15µm, the breaking probability increases remarkably with increased particle diameter.

Therefore, improved mechanical properties can be expected by removing the coarse particles from the reinforcement.

On the other hand, for SiC particle reinforced MMC, it is reported that crack initiation toughness is not influenced by particle size, whereas the tearing modulus, T_{mat}, a parameter of crack growth resistance, can be improved about 2-10 times when the particle size is decreased from 13 µm to 5µm.

Moreover, it is well known that strength and elastic modulus increase with increasing volume fraction of reinforcement. In contrast, elongation and fracture toughness decrease. In such cases, it is reported that the decrease in crack growth resistance such as T_{mat} is more remarkable than the decrease in crack growth initiation toughness.

Kobayashi has simulated crack growth, taking into account the stress shielding effect by microcrack, the crack deflection effect and stress field singularity in DRM of crack growth. Those results clarified that crack propagation resistance could be greatly improved by making the distribution of reinforcement in suitable density, as shown in fig 3.21. In this case, though the degree of the optimum agglomeration differs from volume fraction, crack growth initiation toughness, strength and elastic modulus were not sacrificed by controlling microstructure. That has been confirmed experimentally.

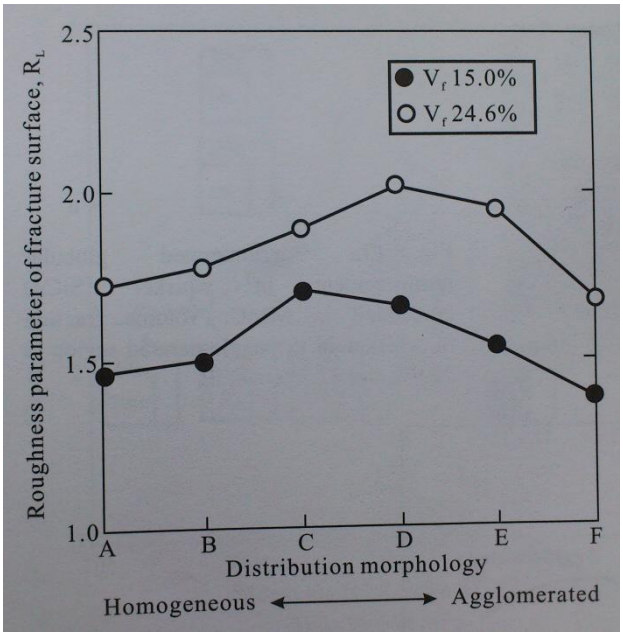

Figure 3.21 Effect of distribution morphology of reinforcement on measure of crack propagation resistance, R_L.

Figure 3.22 shows one example of such MMC reinforced with regular and perfect agglomerated reinforcements. The load-displacement curve for MMC with the reinforcement agglomerates is shown in figure 3.23, where the ductility has been greatly improved. Meanwhile, Kobayashi also attempted an FEM analysis, with results shown in fig 3.24. The result suggest that there is an optimum value for the agglomeration degree for reinforcements [Kobayashi, 2004].

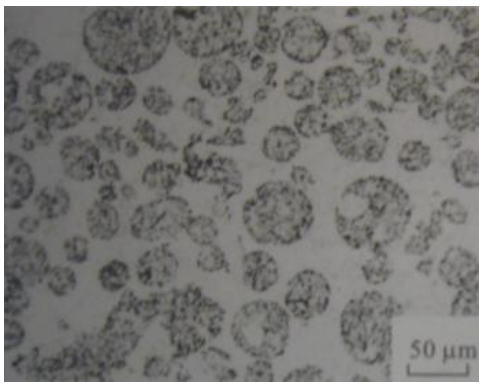

Figure 3.22 Aglomerated globular reinforcement of whisker (SiC_w) embedded in MMC. Volume fraction of whisker in the agglomerated region is 22.9% and 12.3% overall.[Kobayashi 2004].

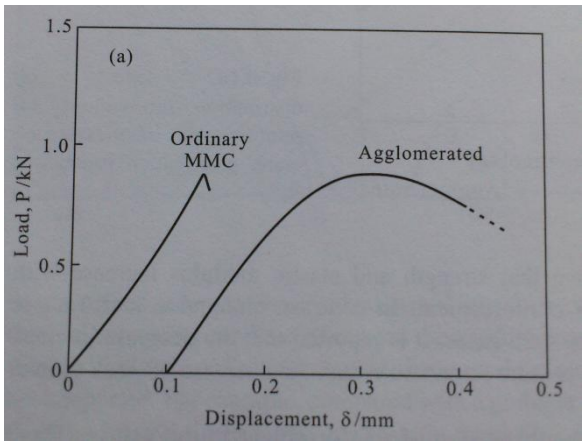

Figure 3.23. Load-displacement curves (three-point bending) of ordinary (homogeneous) and agglomerated MMCs[Kobayashi 2004].

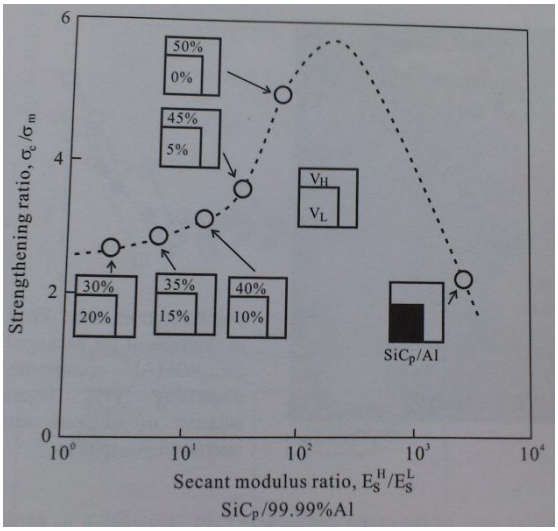

Figure 3.24 The ratio of composite to matrix strength as function of ratio of secant Young's modulus of reinforcing phase (V_H: SiCp%) to softer phase (V_L:SiCp%) for given composite (Al 99.99%-SiC 25%) and overall strain (1%). Reinforcing phase was arranged in a network state in this model.

3.5.2. Microstructural factors about interfaces

Reaction layers likely to form in this MMC interfaces when exposed to high temperature during the manufacturing and heat treatment processes.

First, though interface debonding can be controlled and strength will be increased with strengthening interface, as shown in Fig 3.7, it is reported that in a case of specific damage mechanism, ductility can be improved by decreasing interface strength without decreasing overall strength.

On the other hand, when the elastic modulus of reinforcement is lower than that of the matrix, the reinforcement tends to fail as a result of the increased internal stress. Therefore, it was concluded that a medium elastic modulus is desirable. Moreover, a thermal expansion coefficient of the interface layer that is lower than that of the reinforcement is desirable because axial stress on the interface becomes compressed or has low level tension.

3.5.3. Microstructural factors about the matrix

Generally, residual stress caused by the difference in thermal expansion coefficient between reinforcement and matrix strongly influences strength or toughness of MMC, except for the special case of interface debonding. According to FEM analysis results, Suresh reported that the hydrostatic stress can be relieved by the thermal residual stress under a load corresponding to about 10% yield stress, which leads to a decrease in the apparent Young's modulus of the composite. This tendency was found to be more remarkable under compression loading. Moreover, Ho reported that the thermal residual stress decreases with increasing volume fraction of reinforcement or decreasing the cooling rate.

It is known that the damage mechanism and fracture toughness can be greatly influenced by age hardening for MMC.

The influence of such an alteration matrix surrounding reinforcement on deformation and fracture characteristics has also been examined. As shown in fig 3.25, in a wide range of matrices, larger scale plastic deformation occurs at low load step by existence of PFZ layer, whose thickness is only about 1/10-1/5 of the reinforcement diameter. On the other hand, a remarkable decrease of strength is induced because both void nucleation and growth are promoted by existence of the altered matrix.

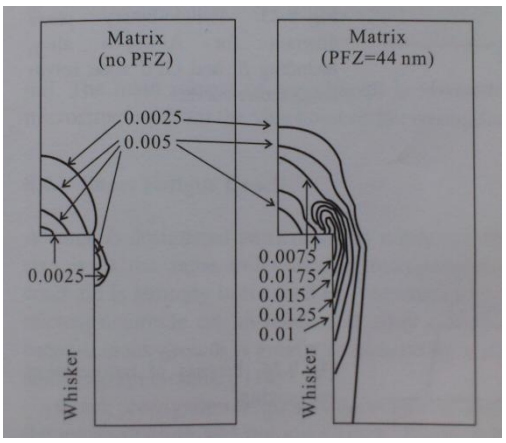

Figure 3.25 Effect of existence of the PFZ layer on distribution of effective plastic strain in the matrix. Results of the FEM analysis using a quarter model of the cell containing a single whisker (1/4 model) [Kobayashi 2004].

Kobayashi has proposed a method for optimizing mechanical properties of MMC by controlling age precipitation microstructure of such a matrix. As shown in fig 3.26, the purpose of the treatment is to homogenize distribution of precipitates, where precipitate-rich and solute-atom-poor areas are resolution-treated by retrogression within 10 seconds to several minutes after solution treatment and the first aging treatment; finally re-again is applied. Strength can be improved about 10% without reducing ductility through application of such RRA (Retrogression and Reaging) treatment [Kobayashi 2004].

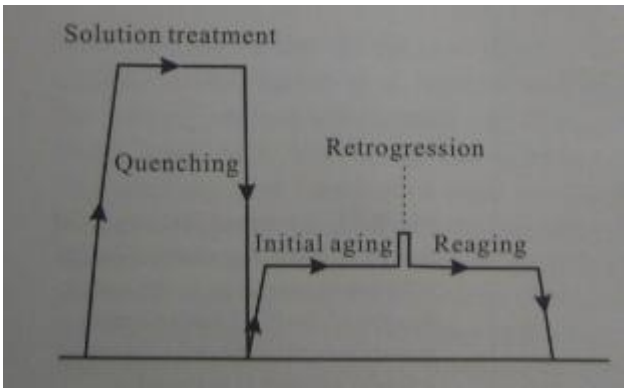

Figure 3.26 Process of retrogression and reaging.

3.6. Residual stresses

The manufacturing processes in MCC can produce significant residual stresses.

This is the case, for example, the sudden cooling (cooling rates in the range of 20 to 500 K/s) to which is subjected the material after extrusion. Here, the different cooling rate.

Moreover, the matrix and the reinforcement are usually different in thermal expansion coefficient. This fact implies that when the PRC is subject to changes of temperature thermal stress generated between both components.

The magnitude of the residual stresses depend, among other variables, the volume fraction of reinforcement, the size and geometry of this, the initial and final temperatures of the process, and the cooling rate. Residual stresses influence the mechanical behavior of PMMC, can alter the values of the yield strength and tenacity. Other effects that are associated with the residual stresses are reduced fatigue resistance, and corrosion shape distortion [Zahr J.(2010)].

4.Fatigue behavior

4.1. Deformation mechanism

When a material is tested cyclically, with amplitude of deformation constant, the stress required to achieve the imposed deformation varies along the deformation process cyclically. This transient state is the cyclic response of the material. During this stage the material can harden or soften, increasing or decreasing the stresses in it appear to maintain the imposed deformation.

After this transitory state is reached a saturation stress. The representing of the half-amplitude of the stress versus saturation half-amplitude of the imposed strain is the cyclic stress-strain curve of the material. (Laird 1975, Dieter 1988 y Suresh 1991)

The behavior under cyclic loading is very sensitive to microstructure factors. When we study the cyclical response of the MMC is important to consider the microstructural changes that appear in the matrix due of the effect of ceramic reinforcement. The presence in the material of the precipitates, shear or no shear by dislocations resulting different mechanisms of cyclic deformation, that correspond with different structures of dislocation in each case.

The alloys hardened by coherent precipitates, shear by dislocations, harden rapidly during cyclic deformation. By continuing the cycles of deformation may appear a region of hardening slower and in some cases it is possible to observe a softening region before rupture occurs. The hardening observed in this type of alloys is justified by the increase in the dislocation density and the subsequent interaction between them. By continuing the deformation of the material, the dislocations form bands of deformation or persistent slip bands as sheared precipitates. The softening observed in some cases often justified by the stripping of coherent precipitates after being repeatedly sheared (Calabrese 1974 and Laird 1975).

Comparing the curves stress-strain monotone and cyclic of the MMC appears a important influence of the heat treatment. In materials aged at room temperature can see an important hardening by cyclic deformation, whereas that the materials aged at high temperature have a stable behavior or even can be seen softening by cyclic strain. (Llorca 1994 , Poza 1995 and Llorca 1995).

The cyclic response and the curve stress-strain cyclical of the MMC also can be understood from the mechanics of the means continuous. In this sense, the analysis by the method of the finite elements of a unit cell representative of the compound has been used to study the mechanical behavior under cyclic loading of the MMC (Llorca 1992 and Llorca 1994).

These analyzes have shown the accumulation of the plastic deformation in the matrix during the process of cyclic deformations of the compounds. These plastic deformations are concentrated initially on the matrix-reinforcement interface, extending progressively to the matrix. The hardening by plastic deformation accumulated in the matrix throughout the process results in a cyclic hardening of the compound, and the MMC reached the saturation stress when the matrix become full of strain hardening. The hardening by cyclic strain of the MMC will be greater the greater the ability of strain hardening of the matrix. (Llorca 1992 and Llorca 1994). The ability of hardening during plastic deformation of the aged materials to room temperature is higher than the materials aged to high temperature, as a result of the different nature of the precipitates.

4.2. Failure mechanism

When a material is subjected to the action of cyclic loading, breakage occurs for values of the stress lower than those which cause the rupture of the material when producing with monotonous load.

When MMC are submited to cycles of amplitude of high strain, the rupture occurs abruptly by similar mechanisms to those described by analyzing stress cracking monotonous load: ductile fracture of the matrix, decohesion of the matrix-reinforcement interface or brittle fracture of the ceramic reinforcement. The ductile failure of the matrix has been described in materials based on alloys with a large population of intermetallic large (Llorca 1992), whereas that in alloys reinforced with whiskers normally, was observed damage by decohesion at the ends of the reinforcement where shows a high concentration of plastic deformations (Allison 1993). In the case of commercial alloys reinforce with ceramic particles, the dominant mechanism of breakage has been the fracture of the ceramic reinforcements. When the strain amplitudes are reduced the number of cycles required to produce rupture of the material, N_t, is the sum of the nuclear cycles required for a crack, N_i, more cycles needed to propagate the crack to rupture that, N_p:

$$N_t=N_i+N_p$$

4.3. Microstructure

The main subject of this chapter is to describe the influence and controlling microstructure from the viewpoint of improving fatigue characteristics.

- Short fatigue crack

A crack is designated particularly as a microstructural short crack when the crack size is in the same order of the microstructure because slip deformation at a crack tip is strongly influenced by microstructure.
Crack propagation frequently decreases or arrests because of interaction between the microstructure and the main crack.

- Long fatigue crack

Firstly, as the influential factors on the intrinsic crack growth resistance in DRM near threshold stress intensity factor range, there are dislocation microstructure or aged precipitation microstructure and crack trapping, as well as the crack deviation (deflection) caused by crack trapping.

Figure 4.1 shows the effect of reinforcement diameter on the crack growth rate in SiC particle reinforced 7091 alloy reported by Ritchie. This result indicates that large diameter particles cause effective crack trapping and increase the degree of crack deviation while simultaneously increasing the level of crack closure. Therefore, it is necessary to choose reinforcement size carefully because the guideline will be quite different according to where emphasis will be placed among material properties such as strength, fracture toughness, and fatigue behavior.

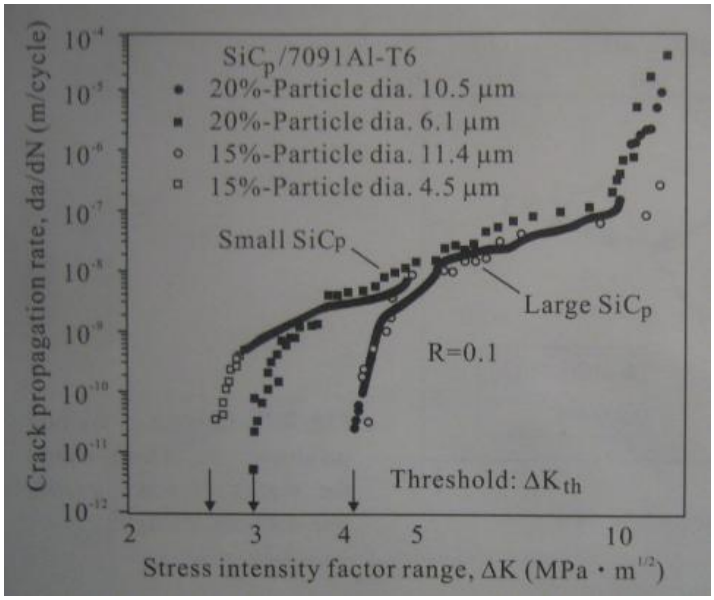

Figure 4.1 Effect of particle size on fatigue crack propagation rate in Al-Zn-Mg-Cu alloy reinforced with SiCp.

Secondly, when a crack grows into the so-called Paris'range, the stable crack growth IIb region, as shown in fig 3.16, the fracture mechanism is similar to static fracture: the main crack is deviated by various stress shielding effects. As a result, the crack grows in a zigzag pattern by merging microcracks. This is shown in fig 4.2. However, in Paris' range of wrought aluminum alloys, cracks develop almost straightly with formation of so-called striations on the fracture surface, which engender smooth fracture surfaces.

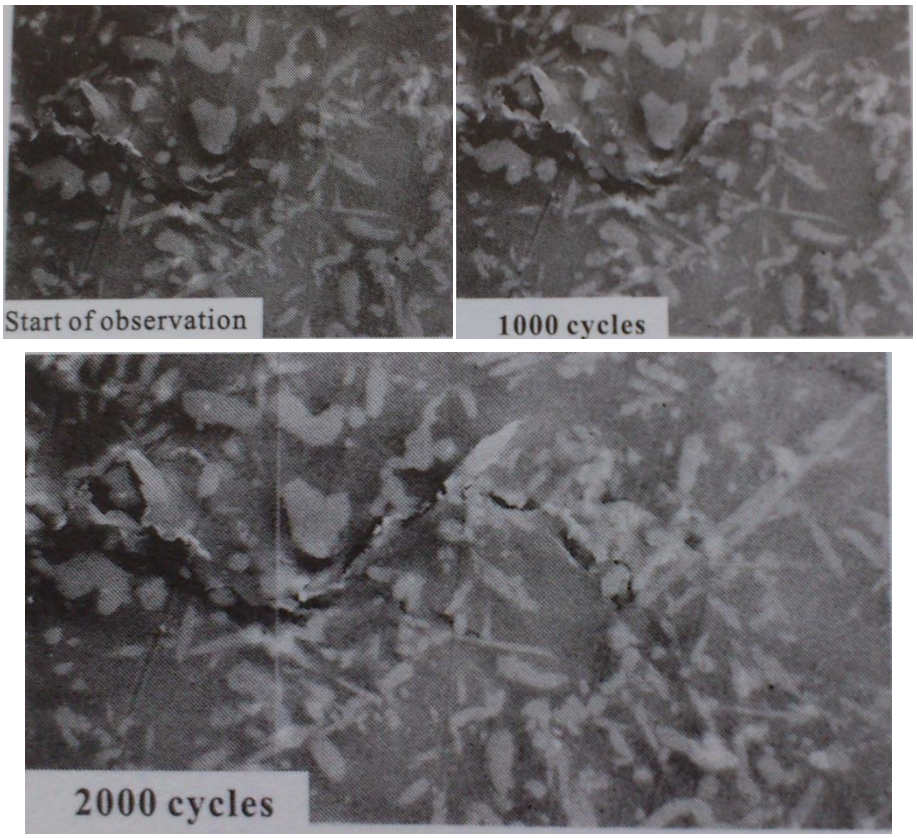

Figure 4.2 Propagation of fatigue crack in the 6061 Al-SiC_w composite (II b stage).

5.References

Allison J. E. y Jones J. W., ”Fatigue behavior of discontinuously reinforce metal matrix composites” in “Fundamentals of metal matrix composites”(1993).

Bao, G., Hutchinson, J. W. and McMeeking, R. M., Acta metal. Mater. (1991).

Brockenbrough, J. R., Suresh, S. and Wienecke, H. A., Acta metal. Mater., (1991).

Brown, L. M. and Stobbs, W. M., Phil Mag. (1976).

Calabrese C. y Laird C. “Cyclic stress-strain response of two phase alloys”(1974).

Corbin, S. F. and Wilkinson, D. S., Acta mettall. Mater.,(1994).

Christman T., Needleman A. y Suresh S., “An experimental and numerical study of deformation in metal-ceramic composites”, Acta Metall. Mater (1989).

Christman, T., Tohgo, K. and Ishii, H., Acta mater (1997).

Derby B. Mummery P. M. y Lawrence C. W., “Characterisation of damage in particle reinforced metal matrixcomposites”, en “Intrinsic and extrinsic fracture mechanisms in inorganic composite systems” (1995).

Derby B. y Walker J. R., “The role of enhanced matrix dislocation density in stngthening metal matrix composites”(1988).

Drucker, D. C., High Strength Materials, ed V. F. Zackay, John Wiley and Sons, New York (1965).

Drucker, D. C., J. of Mater., (1966).

Eshelby, J. D., Proc. Roy. Soc., (1957).

Ghosh, S., Nowak, Z. and Lee, K., Acta mater., (1997).

Garber, R., Ph. D. thesis, Canegie Melon University, Pittsburgh, U.S.A (1981).

He, J., High Spatial Resolution Measurements of the Stress Distribution in Fiber Composites, Ph.D. thesis, University of California, Santa Barbara, U.S.A. (1996).

Kobayashi T. "Strength and Toughness of Materials"(2004).

Levy, A. and Papazian, J. M., Metall. Trans., (1990).

Llorca J., Needleman A. y Suresh S., "An analysis of the effects of matrix void growth on deformation and ductility in metal-ceramic composites", Acta Metall. Mater (1991).

Lloyd D. J., Aspects of Fracture in Particulate Reinforced Metal Matrix Composites, Acta Metall. Mater., (1991).

Lloyd D. J., "Particulate reinforced aluminum and magnesium matrix composites", Int. Mater. Rev (1994).

Llorca J., "The cyclic stress-strain curve of discontinuously-reinforced Al and Mg-based composites" (1994).

Llorca J., Martin A., Ruiz J. y Elices M., "Particulate fracture during deformation of a spray formed metal matrix composite!, Metall. Trans (1993).

Lloyd D. J., Aspects of Fracture in Particulate Reinforced Metal Matrix Composites, Acta Metall. Mater (1991).

Muskhelishvili, N. I., Some Basic Problems of the Mathematical Theory of Elasticity, translated by J. R. M. Rodok, P. Noordhoff Ltd., Groningen, The Netherlands (1963).

Needleman A., Nutt S. R., Suresh S. y Tvergaard V., "Matrix, reinforcement and interfacial failure", in "Fundamentals of metal matrix composites" (1993).

Pedersen, O. B., Acta metal., (1983).

Poole, W. J., Embury, J. D., MacEwen, S. and Kocks, U. F., Phil. Mag., (1994).

Poza P. y Llorca J., "Mechanical behavior and failure micromechanisms of Al/Al_2O_3 composites under cyclic deformation", Metall. Trans., (1995).

Shen, Y. L., Finot, M., Needleman, A. and Suresh, S., Acta metal. Mater., (1995)
Singh P. M. y Lewandowski J. J., "Effects of heat treatment and reinforcement size on reinforcement fracture during tension testing of a SiC_p discontinuously reinforced aluminum alloy", Metall. Trans.,(1993).

Tvergaard, V., Proc IUTAM Symp. On microstructure-property correlation in composite materials, ed. R. Pyrz, Kluwer Pub., Netherlands,(1995).

Tanaka, K. and Mori, T., J. Elasticity (1972).

Thomason, P. F., Acta metall (1985).

Thomason, P. F., Ductile Failure of Metals, Pergamon Press, Oxford (1990).

Van Stone R. H., Cox T. B., Low J. R. y Psioda J. A., "Microstructural aspects of fracture by dimpled rupture ", Inter Metals (1985).

Watt, D. F., Xu, X. Q. and Lloyd, D. J., Acta mater (1996).

Wilkinson, D. F., Maire, E. and Embury, J. D., Mater. Sci. Eng.,(1997).

Wu Y. and Lavernia E. J., "Strengthening behavior of particulate reinforced MMCs", Scripta Met. (1992).

Zahl, D. B., Schmauder, S. and McMeeking, R. M., Acta metal. Mater (1994).

Zahr J. A. "Comportamiento mecánico de materiales compuestos de matris metálica y refuerzo de partículas. Un enfoque basado en celdas multiparticulas"(2010).

Zho D., Tuler F. R. y Lloyd D. j., "Fracture at elevated temperatures in a reinforced composite", Acta Metall. Mater (1994).

Fecha de lectura: Cracovia a 21 de Enero de 2013

Autor: Verónica Torrijos Berlanas

Director de proyecto: Ryszard Pecherski

Cotutor UC3M: Carlos Santiuste

Coordinador académico: Marta Argüeso

Centro en el que se ha realizado el proyecto: AGH

Calificación: 10